



THE UNIVERSITY *of* EDINBURGH

## Edinburgh Research Explorer

### **Maturation of the infant respiratory microbiota, environmental drivers and health consequences: a prospective cohort study**

**Citation for published version:**

Bosch, AATM, de Steenhuijsen Piters, WAA, van Houten, MA, Chu, MLJN, Biesbroek, G, Kool, J, Pernet, P, de Groot, P-KCM, Eijkemans, MJC, Keijser, BJF, Sanders, EAM & Bogaert, D 2017, 'Maturation of the infant respiratory microbiota, environmental drivers and health consequences: a prospective cohort study', *American Journal of Respiratory and Critical Care Medicine*, vol. 196, no. 12, pp. 1582-1590.  
<https://doi.org/10.1164/rccm.201703-0554OC>

**Digital Object Identifier (DOI):**

[10.1164/rccm.201703-0554OC](https://doi.org/10.1164/rccm.201703-0554OC)

**Link:**

[Link to publication record in Edinburgh Research Explorer](#)

**Document Version:**

Peer reviewed version

**Published In:**

American Journal of Respiratory and Critical Care Medicine

**Publisher Rights Statement:**

Author's peer reviewed manuscript as accepted for publication.

**General rights**

Copyright for the publications made accessible via the Edinburgh Research Explorer is retained by the author(s) and / or other copyright owners and it is a condition of accessing these publications that users recognise and abide by the legal requirements associated with these rights.

**Take down policy**

The University of Edinburgh has made every reasonable effort to ensure that Edinburgh Research Explorer content complies with UK legislation. If you believe that the public display of this file breaches copyright please contact [openaccess@ed.ac.uk](mailto:openaccess@ed.ac.uk) providing details, and we will remove access to the work immediately and investigate your claim.



1 **Title:** Maturation of the infant respiratory microbiota, environmental drivers and health  
2 consequences: a prospective cohort study

3

4 **Authors:** Astrid A.T.M. Bosch<sup>1,2†</sup>, Wouter A.A. de Steenhuijsen Piters<sup>1,3,4†</sup>, Marlies A. van  
5 Houten<sup>2</sup>, Mei Ling J.N. Chu<sup>1,3</sup>, Giske Biesbroek<sup>1,2</sup>, Jolanda Kool<sup>5</sup>, Paula Pernet<sup>6</sup>, Pieter-Kees  
6 C.M. de Groot<sup>6</sup>, Marinus J.C. Eijkemans<sup>7</sup>, Bart J.F. Keijser<sup>5,8</sup>, Elisabeth A.M. Sanders<sup>1</sup> and  
7 Debby Bogaert<sup>1,3,4\*</sup>

8

9 † These authors contributed equally to this work.

10 \* Corresponding author. Email: D.Bogaert@ed.ac.uk. Telephone: 0131 242 6582.

11

## 12 **Affiliations**

13 <sup>1</sup> Department of Paediatric Immunology and Infectious Diseases, Wilhelmina Children's  
14 Hospital/University Medical Center Utrecht, Lundlaan 6, 3584 EA, Utrecht, The Netherlands.

15 <sup>2</sup> Spaarne Gasthuis Academy, Spaarnepoort 1, 2134 TM Hoofddorp, The Netherlands.

16 <sup>3</sup> Department of Medical Microbiology, University Medical Center Utrecht, Heidelberglaan  
17 100, 3584 CX Utrecht, The Netherlands.

18 <sup>4</sup> Medical Research Council/University of Edinburgh Centre for Inflammation Research,  
19 Queen's Medical Research Institute, University of Edinburgh, 47 Little France Crescent, EH16  
20 4TJ Edinburgh, United Kingdom.

21 <sup>5</sup> Microbiology and Systems Biology Group, Netherlands Organisation for Applied Scientific  
22 Research (TNO), Utrechtseweg 48, 3704 HE Zeist, The Netherlands.

23 <sup>6</sup> Department of Obstetrics and Gynaecology, Spaarne Gasthuis, Spaarnepoort 1, 2134 TM  
24 Hoofddorp, The Netherlands.

25 <sup>7</sup> Biostatistics and Research Support, Julius Center for Health Sciences and Primary Care,  
26 University Medical Center Utrecht, Universiteitsweg 100, 3584 CG Utrecht, The Netherlands.

27 <sup>8</sup> Department of Preventive Dentistry, Academic Center for Dentistry Amsterdam (ACTA),  
28 University of Amsterdam and Vrije University Amsterdam, Gustav Mahlerlaan 3004, 1081 LA  
29 Amsterdam, The Netherlands.

30

### 31 **Author contributions**

32 MAvH, EAMS, and DB designed the experiments, AATMB, MAvH, GB, EAMS, and DB  
33 wrote the study protocols. AATMB, PP and PCMdG were responsible for patient recruitment.  
34 AATMB and MAvH were responsible for clinical data collection. MLC was responsible for  
35 sample preparation and MLC, JK, and BK for 16S-rRNA gene amplicon sequencing.  
36 WAAAdSP, MJCE and DB were responsible for bioinformatic processing and statistical  
37 analyses. WAAAdSP, AATMB, and DB wrote the paper. All authors significantly contributed to  
38 interpreting the results, critically revised the manuscript for important intellectual content, and  
39 approved the final manuscript.

### 40 **Funding**

41 This work was supported in part by The Netherlands Organisation for Health Research and  
42 Development (ZonMW; grant 91209010); The Netherlands Organisation for Scientific research  
43 (NWO-VIDI; grant 91715359); Wilhelmina Children's Hospital and Spaarne Gasthuis  
44 Hoofddorp intramural funds; and Topconsortia for knowledge and innovation (Agri & Food;  
45 TKI-AF-12190).

46

47 **Running title:** Early-life respiratory microbiota development related to infections

48

49 **Descriptor:** 10.11 Pediatrics: Respiratory Infections

50

51 **Total word count:** 4,483/3,500 words.

52

53 **Word count abstract:** 260/250 words.

54

55 **At a glance commentary**

56 *What is the current scientific knowledge on this subject?*

57 Factors affecting the risk of respiratory tract infections have been well characterized, however  
58 it is unknown how these factors might impact respiratory microbiota development and thereby  
59 susceptibility to respiratory tract infections (RTIs). Studies in mice suggest that timely  
60 microbial cues contribute to healthy immune development, in turn enforcing the defense against  
61 invading respiratory pathogens.

62

63 *What does this study add to the field?*

64 Using a longitudinal study design and high sampling resolution, we characterized the  
65 nasopharyngeal microbiota maturation over the first year of life in 112 infants both during  
66 health (11 sampling moments) and at the moment of RTIs. We observed differences in the  
67 microbial community maturation in children who ultimately became more susceptible to  
68 infections compared to children who were more resistant to infections. These changed dynamics  
69 were related to shifts in the abundance of specific members of the microbiota and environmental  
70 factors that are known to impact susceptibility to RTIs, such as mode of delivery, mode of  
71 feeding, early antibiotic use and crowding. Altered microbiota maturation was evident from the  
72 first month of life on and preceded factual RTIs, strongly suggesting that early-life microbiota  
73 development impacts long-term respiratory health.

74

75 This article has an online data supplement, which is accessible from this issue's table of content

76 online at [www.atsjournals.org](http://www.atsjournals.org)

77

78

79

80

81 **Abstract**

82 **Rationale:** Perinatal and postnatal influences are presumed important drivers of the early-life  
83 respiratory microbiome composition. We hypothesized that the respiratory microbiome  
84 composition and development in infancy is affecting microbiome stability and thereby  
85 resilience against respiratory tract infections (RTIs) over time.

86 **Objectives:** To investigate common environmental drivers, including birth mode, feeding type,  
87 antibiotic exposure and crowding conditions, in relation to respiratory tract microbiota  
88 maturation and stability, and consecutive risk of RTIs over the first year of life.

89 **Methods:** In a prospectively followed cohort of 112 infants, we characterized the  
90 nasopharyngeal microbiota longitudinally from birth on (11 consecutive sample moments and  
91 maximum three RTI samples per subject; in total  $n=1,121$  samples) by 16S-rRNA gene  
92 amplicon sequencing.

93 **Measurements and Main Results:** Using a microbiota-based machine-learning algorithm we  
94 found that children experiencing a higher number of RTIs in the first year of life demonstrate  
95 an aberrant microbial developmental trajectory already from the first month of life on as  
96 compared to the reference group (0-2 RTIs/year). The altered microbiota maturation process  
97 coincided with decreased microbial community stability, prolonged reduction of  
98 *Corynebacterium* and *Dolosigranulum.*, enrichment of *Moraxella* already very early in life,  
99 followed by later enrichment of *Neisseria* and *Prevotella* spp. Independent drivers of these  
100 aberrant developmental trajectories of respiratory microbiota members were mode of delivery,  
101 infant feeding, crowding and recent antibiotic use.

102 **Conclusions:** Our results suggest that environmental drivers impact microbiota development  
103 and consequently resilience against development of RTIs. This supports the idea that microbiota  
104 form the mediator between early life environmental risk factors for and susceptibility to RTIs  
105 over the first year of life.

106 **Key words:** respiratory microbiota, nasopharynx, respiratory tract infections, development,  
107 risk factors.  
108

109 **Introduction**

110 Acute respiratory tract infections (RTI) are a leading cause of childhood mortality, being  
111 responsible for ~0.9 million yearly deaths (15.5% of all deaths) worldwide in children <5 years  
112 (1). In addition, these infections are associated with significant morbidity (2) and are a major  
113 reason for antibiotic prescription (3), especially in young children. Although it is still unclear  
114 why one individual is more vulnerable to respiratory infections compared to another, it was  
115 previously hypothesized that - besides environmental and host-related influences - the  
116 respiratory microbiota may modulate susceptibility to disease.

117  
118 Directly after birth, the mucosal surfaces of the respiratory tract of neonates are rapidly  
119 colonized with a variety of microbiota, that are swiftly moulded into niche-specific bacterial  
120 communities (4, 5). Over the first months to years of life, these communities are highly dynamic  
121 and heavily influenced by environmental factors, including mode of delivery (4, 6), season (7),  
122 feeding type (8), and antibiotic treatment (9). In previous studies we found that the microbial  
123 composition at the age of six weeks was indicative of microbiota stability and RTI susceptibility  
124 over the first two years of life (10, 11). This finding underscores the importance of direct  
125 postnatal environmental influences and subsequent early microbiota maturation on future  
126 respiratory health.

127  
128 The healthy human respiratory microbiome is assumed to stimulate immune maturation (12,  
129 13), promote epithelial integrity (14), and provide colonization resistance (15), thereby  
130 preventing overgrowth and invasion of potential pathogenic bacteria (16). In contrast,  
131 deviations from a healthy bacterial respiratory community composition have been associated  
132 with susceptibility to and/or severity of childhood respiratory diseases, including acute otitis



133 media (17, 18), respiratory syncytial virus (RSV) disease (19) and asthma development (20) in  
134 various retrospective and cross-sectional studies (21).

135

136 We here postulate that alterations in the respiratory microbiome development early in life are a  
137 consequence of changes in the abundance of specific bacterial biomarkers species. We  
138 hypothesize that these alterations are controlled by known host-related and environmental  
139 influences, and can ultimately lead to altered microbiota stability, in turn affecting RTI  
140 susceptibility. Therefore, we prospectively investigated the nasopharyngeal microbiota  
141 maturation of 112 unselected, healthy children with frequent, short interval sampling during the  
142 first year of life as well as during RTI episodes. Hereby, we aimed to study respiratory  
143 microbiota development early in life, and investigate its role as potential mediator between  
144 early-life drivers and susceptibility to respiratory infectious disease.

145

146

## 147 **Methods**

148 Details on the study design, sample and data collection and bioinformatics/statistical methods  
149 can be found in the online supplement Methods. Data have been deposited in the National  
150 Center for Biotechnology Information GenBank database (accession number: SRP093519).

### 151 *Study population*

152 We enrolled in total 128 healthy children in an ongoing prospective birth cohort study aiming  
153 to investigate the development of the infant microbiome during health and disease. Of 128  
154 infants, 12 children were lost to follow-up (Figure E1). Details on the trial methods have been  
155 described elsewhere (4). Written informed consent was obtained from both parents. The study

156 was approved by the Ethics Committee of Noord Holland, The Netherlands (M012-015,  
157 NH012.394, NTR3986). Sequence data of part of the samples ( $\leq 6$  months;  $n=743$  samples of  
158 101 children) were used for a study on the role of mode of delivery on respiratory microbiota  
159 acquisition (4).

#### 160 *Data collection*

161 For the current analyses, we included samples and data of 112/116 children who completed the  
162 one-year follow-up and for whom we had  $\geq 8$  samples available for further analyses after  
163 laboratory work-up (Figure E1). Home visits were conducted within two hours after birth, at  
164 24 hours, at seven and 14 days, and at one, two, three, four, six, nine, and 12 months of age.  
165 During each home visit, a trained doctor or research nurse obtained a nasopharyngeal swab  
166 according to World Health Organization protocol (22) and completed an extensive survey on  
167 the health status of the child, as well as on the presence or absence of potential risk and  
168 environmental factors related to respiratory disease (4). Next to these regular visits, parents  
169 were asked to contact the study team in case of an active RTI, defined as fever  $\geq 38^{\circ}\text{C}$  for  $>6$   
170 hours combined with malaise and presence of RTI symptoms. Following, a RTI visit was  
171 planned within 48 hours after start of the fever to collect additional samples and to obtain more  
172 detailed medical information.

#### 173 *16S-rRNA gene amplicon sequencing*

174 Bacterial DNA of the nasopharyngeal samples was isolated, amplicon libraries of the 16S-  
175 rRNA gene (V4 region) were generated, and sequencing was executed as previously described  
176 (4, 23). Amplicon pools were paired-end sequenced in eight runs using an Illuminia MiSeq  
177 instrument (Illumina Inc., San Diego, CA, USA). Bioinformatic processing included trimming,  
178 error correction, assembly and 97%-identity clustering of reads into OTUs. Following removal

179 of chimeric reads, OTUs were taxonomically annotated using SILVA and BLASTN (Table E1).  
180 We refer to OTUs using maximum genus level annotations, combined with a rank number based  
181 on the abundance of each given OTU. Details on processing and quality control, including the  
182 use of negative controls, are described in the online supplement Methods. After abundance-  
183 filtering, a rarefied dataset was generated, and used for downstream analyses (24).  $\alpha$ -diversity  
184 measures were averaged over 100 rarefactions.  $\beta$ -diversity was assessed using the Bray-Curtis  
185 dissimilarity metric.

### 186 *Statistical analysis*

187 All analyses were performed in the R version 3.3.0 within R studio version 0.99.902.

### 188 *Random forest analysis*

189 We hypothesized that the nasopharyngeal microbial succession patterns would be altered in  
190 children who experienced more RTIs during their first year of life. Therefore, we stratified our  
191 population into three groups based on the normal distribution of RTIs over the first year of life  
192 (Figure E2); 39 children with 0-2 RTIs (reference group;  $n=372$  samples), 52 children with 3-  
193 4 RTIs ( $n=496$  samples) and 21 children with 5-7 RTIs ( $n=197$  samples). To identify OTUs  
194 characteristic of a healthy microbiota maturation, we regressed the relative abundance of all  
195 576 OTUs against chronological age in the reference group using the *randomForest* package,  
196 and selected age-discriminatory OTUs using a step-wise backward 10-fold cross validation  
197 procedure, see online supplement Methods and Figure E3A and E3B (24). This selection of  
198 OTUs was subsequently used as input to a random forest model where we regressed the relative  
199 abundance of these OTUs versus chronological age in the reference group. The resulting final  
200 model was then used to predict chronological age, referred to as ‘microbiota age’, in samples  
201 from individuals who experienced 3-4 and 5-7 RTIs and on the group of samples collected

202 during RTIs ( $n=56$  samples). To generate accurate microbiota age estimates for the reference  
203 group, we used a 10-fold cross-validation procedure. Relative microbiota age (RMA) was  
204 calculated as follows: relative microbiota age = microbiota age of a given child – microbiota  
205 age of the reference group at similar age as determined by a spline fit (24). As a post-hoc  
206 analysis, we studied the effect of the *Moraxella*-genus on the performance of the microbiota  
207 age model by excluding the OTUs belonging to the *Moraxella*-genus from the model while  
208 monitoring the amount of variance explained.

### 209 *Associations between environmental factors and microbiota parameters*

210 ‘Environmental factors’ used in the descriptions of the various models comprises birth mode,  
211 breast feeding until three months of age, day care attendance, presence of siblings >five years  
212 of age, antibiotic treatment in the previous four weeks and season of birth, if not specified  
213 otherwise. If applicable, correction for multiple testing was performed using the Benjamini-  
214 Hochberg procedure.

215 Microbial succession patterns were visualised using non-metric multidimensional  
216 scaling (nMDS; *vegan* package) based on the Bray-Curtis dissimilarity matrix. We performed  
217 two separate analyses based on permutational multivariate analysis of variance  
218 (PERMANOVA)-tests and the Bray-Curtis dissimilarity matrix, to study the effect of 1)  
219 environmental factors, age and subject, and 2) the number of RTIs experienced in the first year  
220 of life, on the overall bacterial community structure. Permutations were constrained within  
221 subjects to account for repeated measures. This analysis was repeated over 100 rarefactions to  
222 assess the robustness of our results based on one rarefied set.

223 To complement the group-based analyses, we also assessed the microbial development  
224 at the individual level using an unsupervised clustering approach. The proportion of samples  
225 within each cluster at each time point was visualised using an alluvial diagram, stratified by the  
226 number of RTIs that children experienced over the first year of life.

227

228 We used separate linear mixed models to assess the associations between (relative) microbiota  
229 age and stability ( $\alpha$ -/ $\beta$ -diversity measures) as dependent variables and 1) environmental factors  
230 and 2) the number of RTIs (fixed effects), while adjusting for age and with the subject-variable  
231 included as a random intercept (*lme4* package). In addition, the relationships between 1)  
232 bacterial density and 2) relative abundance (dependent) and sampling moment (fixed) were  
233 assessed using linear mixed models.

234

235 We used smoothing spline analysis of variance (SS-ANOVA; *metagenomeseq* package) for the  
236 analyses of 1) the differences in abundance of age-discriminatory OTUs between RTI-groups,  
237 and 2) the effects of birth mode and breastfeeding on the nasopharyngeal microbiota, as it  
238 simultaneously tests for the existence and timing of differences in OTU-abundance. To confirm  
239 associations between environmental factors and relative abundance of microbiota in a  
240 multivariable manner, we used the Multivariate Association with Linear Models (MaAsLin)  
241 (R-)package, adjusting for age and with subject as a random effect.

242

243

## 244 **Results**

### 245 *Baseline characteristics of the study population*

246 Baseline characteristics of the study population stratified by number of RTIs experienced in the  
247 first year of life can be found in Table E2.

### 248 *Nasopharyngeal microbiota composition in the first year of life*

249 A median of 20,670 reads were generated per sample (range 3,911-97,870 reads), which were  
250 binned into a total 576 operational taxonomic units (OTUs; after filtering), representing a total  
251 of 14 bacterial phyla. Firmicutes was the most abundant phylum with a maximum abundance  
252 of 65.4% at day one (mainly *Staphylococcus* (3), *Dolosigranulum* (4) and *Streptococcus* (5)).  
253 Later, Proteobacteria emerged and became predominant with a maximum abundance of 71.7%  
254 at 12 months of life (mostly *Moraxella* (1), *Haemophilus* (6) and *Moraxella* (7); Figure 1,  
255 Figure 2 and Figure E4). We observed major shifts in nasopharyngeal microbiota composition  
256 between day 0 and day one and between day one and week one (Figure E5). The difference in  
257 microbiota composition between day one and week one coincided with a strong increase in  
258 absolute bacterial abundance, which then increased up to the age of ~1 month, after which it  
259 stabilized (linear mixed model;  $q < 0.001$ ; Figure 3).

#### 260 *Trajectories of microbial development*

261 We aimed to study whether nasopharyngeal microbiota development is different in infants  
262 experiencing more RTIs in the first year of life compared to the low-burden infants. First, we  
263 demonstrated that the microbial community composition was significantly associated with the  
264 number of RTIs experienced in the first year of life (i.e. 1-7 RTIs; categorical), after adjusting  
265 for age, using a PERMANOVA-test (Table E3A; 1.7% of the variance explained,  $p = 0.001$ ).  
266 Subsequently, we stratified the study participants over three groups based on the number of  
267 RTIs they experienced within the first 12 months of life (i.e. 0-2, 3-4 and 5-7 RTIs; Figure E2  
268 and Table E2). To explore the microbial succession patterns at the individual level, we clustered  
269 samples using an unsupervised clustering approach. The proportion of individuals in each  
270 cluster at each time point was then visualised using an alluvial diagram stratified by the number  
271 of RTIs experienced over the first year of life (figure E6). We identified 8 clusters over all time  
272 points, of which the largest four were enriched for *Moraxella* (1) (MOR1, 38.5% of samples)

273 *Corynebacterium* (2) and *Dolosigranulum* (4) (CDG, 19.7%), *Staphylococcus* (3) (STA,  
274 19.4%) and *Streptococcus* (5) (STR, 8.4%). In concordance with our previous observations, we  
275 found that the CDG-cluster has a much more prominent and prolonged role in the reference  
276 group compared to children who suffered from 5-7 RTIs. Instead, these children appear to ‘skip’  
277 the CDG-cluster altogether, transitioning directly from the early-life STA-cluster to the MOR1-  
278 cluster (figure E6C), the latter of which is typically observed more often at later time points in  
279 the reference cohort (figure E6A). In the children who experience 3-4 RTIs the cluster  
280 distributions at each time point do resemble those of the reference group, although an early rise  
281 of the *Haemophilus* (6) (HAE)-cluster was noted (figure E6B).

282 *Nasopharyngeal microbiota maturation in relation to susceptibility to RTI and identification of*  
283 *age-discriminatory taxa*

284 To further assess these differences in microbiota dynamics we used a random forest regression  
285 model. First, we identified age-discriminatory OTUs in the reference group (i.e. 0-2 RTIs;  
286 Figure E3A and 3B) and regressed their relative abundance against chronological age, enabling  
287 us to model healthy microbiota development (65.9% of variance explained, based on 10-fold  
288 cross-validation, 100 repetitions). Then, the model was used to calculate predicted  
289 chronological age or ‘microbiota age’ in children with 3-4 and 5-7 RTIs and in samples taken  
290 during RTIs (58.1% variance explained), subsequently comparing these estimates to  
291 chronological age. We first observed that children with 5-7 RTIs showed an accelerated  
292 microbiota maturation when compared to the reference group from very early in life on (linear  
293 mixed model;  $p=0.007$ ). A similar, although non-significant trend was observed in children  
294 with 3-4 vs reference group (linear mixed model;  $p=0.13$ ; Figure 4A). The accelerated  
295 microbiota developmental patterns in children with  $>2$  RTIs were related to an early enrichment  
296 of *Moraxella* (1) from just after birth on (SS-ANOVA;  $q=0.007$ ), enrichment of *Neisseria*,

297 *Prevotella* and *Alloprevotella* spp. from month two onwards (SS-ANOVA;  $q \leq 0.021$ ) and  
298 (prolonged) absence of *Corynebacterium* (2) and *Corynebacterium* (80), *Dolosigranulum* (4)  
299 and *Streptococcus* (10) (SS-ANOVA;  $q \leq 0.039$ ; Figure 4B, Figure E7 and Table E4A).  
300 Subgroup analyses comparing either the 3-4 or 5-7 RTI groups to the reference group yielded  
301 highly similar results (Table E4B and E4C).

302 To assess whether the above differences were predominantly driven by the *Moraxella* genus  
303 rather than by the total group of biomarkers species, we assessed the impact of *Moraxella* spp.  
304 on the performance of the microbiota age model by repeating the analyses including all  
305 biomarker OTUs, except those belonging to the *Moraxella*-genus. This model, containing 18  
306 OTUs, showed a confined effect of *Moraxella* spp., with a small reduction of performance in  
307 the reference group (60.9% variance explained) and a slightly improved performance in  
308 children who experienced 3-4 or 5-7 RTIs over the first year of life and in samples taken during  
309 RTI (60.1% variance explained), compared with the model based on 22 OTUs.

#### 310 *Relative microbiota age in relation to (susceptibility to) RTI*

311 By calculating the relative microbiota age (RMA; defined as the difference in microbiota age  
312 between susceptible groups versus the reference group) we verified that microbiota age was  
313 increased in children with 5-7 RTIs compared to the reference group (linear mixed model,  
314 adjusted for age;  $p=0.007$ ; Figure E8), which was already apparent in the first month of life  
315 ( $p=0.011$ ; linear mixed model; post-hoc analysis in children  $\leq 1$  month of age). This latter  
316 finding was substantiated by a PERMANOVA-test, demonstrating that the microbiota  
317 composition over the first month of life was significantly associated with the number of RTIs  
318 over the first year of life (Table E3D; 0.8% of the variance explained,  $p=0.001$ ). The RMA was  
319 not significantly different between the group with 3-4 RTIs and the reference group ( $p=0.12$ ).  
320 Moreover, although the RMA was maximal during RTIs (median RMA +67.8 days in RTI



321 samples), we already observed an increase in RMA during the period preceding the factual RTI  
322 (median RMA +37.1 days at the first time point preceding RTI [T = -1]; p=0.004), suggesting  
323 that the microbiota maturation alterations precede RTIs. After recovery from an RTI, RMA  
324 decreased towards the reference group, though did not normalize (median RMA +29.7 days T  
325 = +1; p=0.04; Figure 4C). Although these changes in RMA appeared to be related to individual  
326 OTUs (figure E9), these changes were not statically significant.

### 327 *Nasopharyngeal microbiota stability over time*

328 We next investigated whether bacterial community stability over time was different for children  
329 who experienced 0-2, 3-4 and 5-7 RTIs over the first year of life. Community stability,  
330 measured by the Bray-Curtis dissimilarity between consecutive time points, was significantly  
331 different between children with 0-2 RTIs and those with 3-4 and 5-7 RTIs (linear mixed model;  
332 p=0.005 and p=0.02, respectively). This phenomenon was apparent from the age of three  
333 months on (Figure 5).

### 334 *Impact of environmental drivers on bacterial community composition*

335 We then aimed to assess the effect of environmental factors on nasopharyngeal microbiota  
336 composition and succession. Using PERMANOVA tests, we found that factors with the largest  
337 impact comprised subject (unadjusted  $R^2=18.7\%$ ), chronological age (10.4%) and  
338 environmental drivers, including presence of siblings <five years of age (1.6%), day care  
339 attendance (0.9%), season of birth (0.7%), breastfeeding for at least three months (0.5%), birth  
340 mode (0.4%) and antibiotic usage in the previous month (0.3%; all p-values  $\leq 0.016$ ; Table E3B  
341 and E3C).

### 342 *Environmental drivers and their effects on microbiota maturation, stability and individual* 343 *bacterial taxa*

344 After showing microbiota maturation is accelerated in children more susceptible to RTIs, we  
345 next set out to determine the influence of environmental drivers on this process. We modelled  
346 the RMA using a linear mixed model including environmental factors. We observed that  
347 particularly the presence of young siblings and day care attendance are associated with an  
348 increased RMA early in life (both  $p < 0.0005$ ). Similar associations were found when directly  
349 modelling microbiota age instead of RMA versus environmental drivers (data not shown). In  
350 contrast, the observed differences in microbiota stability between groups could not be explained  
351 by environmental factors (linear mixed model;  $p > 0.05$ ) and did not relate to differences in  $\alpha$ -  
352 diversity measures between groups (linear mixed model;  $p > 0.05$ , Figure E10). We also did not  
353 detect differences in microbiota stability directly prior to, during or following a RTI episode.

354 We further tested the contribution of individual bacterial taxa to the associations  
355 between environmental factors and microbiota maturation using MaAslin. With respect to age-  
356 discriminatory taxa, we found that *Moraxella* spp. were positively and *Staphylococcus* spp.  
357 were negatively associated with day care (both  $q < 0.0005$ ). Furthermore, we found that  
358 *Corynebacterium* (2) and *Dolosigranulum* (4) were strongly reduced following antibiotic usage  
359 ( $q < 0.03$ ). Additionally, we observed many associations between environmental drivers and  
360 bacterial taxa that were not previously assigned as age-discriminatory biomarkers. Notably, the  
361 presence of siblings was associated with increased abundance of the family *Pasteurellaceae*  
362 ( $q = 0.003$ ), which includes the *Haemophilus* genus (Table E5).

### 363 *Temporal effects of mode of delivery and feeding type on bacterial taxa*

364 Since MaAsLin is not suited to identify temporary effects and the timeframes within which they  
365 occur, we additionally studied the impact of early life drivers, such as mode of delivery and  
366 feeding type, on the microbial succession patterns using SS-ANOVA. Of the age-  
367 discriminatory taxa, early and/or prolonged predominance of *Corynebacterium* (2),

368 *Corynebacterium* (8) and *Dolosigranulum* (4) ( $q \leq 0.03$ ) and late enrichment of *Moraxella* spp.  
369 ( $q < 0.05$ ; from ~month 3 on) were associated with vaginal birth and/or breastfeeding.  
370 Contrariwise, in formula fed and/or caesarian born children we observed a high abundance of  
371 *Gemella* (9) and *Streptococcus* (10) ( $q \leq 0.012$ ) from birth on, and prolonged (4-11 months)  
372 predominance of *Neisseria* spp. and (facultative) anaerobes including (*Allo*)*prevotella*,  
373 *Granulicatella* and *Actinomyces* spp. ( $q < 0.05$ ) after the first month of life. Abundance of the  
374 age-discriminatory taxum *Staphylococcus* (3) was related to birth by caesarian section in the  
375 first month of life only ( $q = 0.016$ ). Besides, although not directly linked to microbiota  
376 maturation, we found that the additional early enrichment of *Streptococcus* (5) was associated  
377 with caesarian section and/or formula feeding (from birth on;  $q \leq 0.026$ ), which could be  
378 confirmed using MaAsLin (Table E5). Additionally, we observed temporal enrichment of oral  
379 type of bacteria including streptococci and facultative anaerobic bacteria like *Prevotella*,  
380 *Porphyromonas* and *Veillonella* spp., in formula fed children (from ~month 1-2 onwards) and  
381 early abundance of *Dolosigranulum* (4) in breastfed children (Table E6 and E7 and Figure E11  
382 and E12).

383

384

## 385 **Discussion**

386 Microbial colonization of the upper respiratory tract occurs directly after birth and develops  
387 rapidly towards niche-specific profiles during the first weeks of life (4, 5, 10, 25). Several cross-  
388 sectional case-control studies have shown differences in respiratory microbial profiles between  
389 children with and without acute otitis media (18, 26), and between infants with mild, moderate  
390 and severe RSV (19). Longitudinal studies, linking respiratory microbiota development and

391 maturation and (risk of) RTIs, however, are sparse, lack detailed information, and are only  
392 retrospectively executed (10, 20).

393

394 Our results suggest that microbiota maturation in healthy children who experience a limited  
395 number of 0-2 RTIs in the first year of life (reference group), is associated with a specific timing  
396 of colonization events accompanied by the consecutive appearance and disappearance of  
397 specific community members. In general, we observed that during the first week of life, the  
398 microbiota development is typified by a strong increase in absolute bacterial abundance. In the  
399 reference group, this coincides with the initial expansion of *Streptococcus* spp. at day one,  
400 supplanted by rapid niche-differentiation at one week of life, initially driven by staphylococcal  
401 predominance, but quickly followed by the establishment of multiple *Corynebacterium* and  
402 *Dolosigranulum* spp.: a process which is strongly related to vaginal delivery (4) as well as  
403 breastfeeding. Although *Moraxella* spp. become predominant community members over time  
404 in most children, in the reference group they only become the main community members from  
405 2-3 months of life on. From that age on, *Moraxella* spp. may still co-occur with  
406 *Corynebacterium* and *Dolosigranulum* spp. in a mixed community profile or they can truly  
407 dominate all other community members in a *Moraxella* spp. dominated community profile (4).  
408 This natural process of consecutive events coincides with normalization of ecological stability  
409 from the age of three months on and fewer infections.

410 In contrast, children with high susceptibility to RTIs over the first year of life exhibit an  
411 accelerated bacterial community maturation from as early as the first month of life on, i.e. prior  
412 to development of their first RTIs. This pattern was characterised by diminished and less  
413 prolonged establishment of *Corynebacterium* and *Dolosigranulum* spp. coinciding with  
414 premature predominance of *Moraxella* spp. colonization, and more abundant and prolonged  
415 presence of oral types of bacteria in the nasopharyngeal niche, including *Neisseria* and

416 *Prevotella* spp. The observed aberrant microbial succession in children with more RTIs also  
417 coincided with decreased bacterial community stability over time, which is in line with previous  
418 observations and support the ecological theory that more stable microbiota are more resistant  
419 to RTIs (10). Interestingly, we could also show that acceleration of microbiota age preceded  
420 the factual RTIs, supporting the hypothesis that microbiota changes forego a clinically  
421 symptomatic RTI. Conjointly, these findings support our hypothesis that the initial early  
422 colonization after birth and subsequent development of URT microbiota over the first months  
423 of life impact respiratory health.

424

425 Our data, in line with others, show that prolonged abundance of *Corynebacterium* and  
426 *Dolosigranulum* spp. are linked to healthy microbiota development and microbiota stability  
427 (10, 17, 20, 26), and are related to breastfeeding and vaginal delivery (4, 8, 27). Their co-  
428 occurrence may be explained by the ability of *Dolosigranulum* spp. to produce lactic acid,  
429 which plausibly selects for *Corynebacterium* spp. outgrowth (21). Antagonism between  
430 *Corynebacterium* spp., and *Streptococcus pneumoniae*, a known respiratory pathogen, may at  
431 least in part explain their association with respiratory health (17, 26, 28). Since we and others  
432 (20, 29) showed that antibiotic use in infancy is associated with depletion of *Corynebacterium*  
433 and *Dolosigranulum* spp., routinely used antibiotics may therefore have more (prolonged)  
434 consequences for microbiota-driven resilience against RTIs than currently is thought.

435         Conversely, accelerated microbial succession patterns in children with more RTIs were  
436 characterized by enrichment of *Neisseria* spp. and (facultative) anaerobic, mainly oral species,  
437 including *Prevotella* spp., which in turn were linked to formula feeding. Similar findings have  
438 been reported previously (10, 30), and imply a loss of topography within the upper respiratory  
439 tract, suggesting that the host or the local ecosystem is unable to restrain oral microbiota within

440 their niche early in life. As presence of these bacteria is linked to RTI susceptibility, further  
441 studies on their role in respiratory health is warranted.

442 In literature, conflicting results have been reported regarding the role of *Moraxella* spp.  
443 in the pathogenesis of RTIs. Some studies found that *Moraxella* spp. colonization was  
444 associated with respiratory infections including pneumonia and bronchiolitis (11), while others  
445 reported that the *Moraxella*-dominated profile was associated with bacterial community  
446 stability (10, 20) and fewer RTI episodes (10). Although in our study, development from a  
447 *Staphylococcus*- into a *Corynebacterium/Dolosigranulum*-, towards a *Moraxella*-dominated  
448 profile eventually occurs in the great majority of children, we here show that especially lack of  
449 *Corynebacterium/Dolosigranulum* spp. establishment coincides with a premature transition  
450 from *Staphylococcus*- towards a *Moraxella*-dominated profile, which is associated with influx  
451 of oral bacterial species and an increased risk of RTIs (20). In line, several studies in mice have  
452 demonstrated that the neonatal immune system requires cues from the respiratory microbiota  
453 for its development within a specific time frame (12, 13). Indeed, premature *Moraxella* spp.  
454 colonization is shown to induce a mixed pro-inflammatory immune response (31), although  
455 data on the effects of *Moraxella* spp. colonization at later age are lacking. In addition, it  
456 deserves further study whether the required microbial triggers might be species and/or strain  
457 specific.

458  
459 In our prospective, birth cohort study we collected frequent nasopharyngeal samples of a large  
460 number of healthy children at regular intervals over the first year of life as well as during RTIs,  
461 allowing us to study the microbial development during health, preceding and during RTI  
462 episodes. More importantly, it allowed us to explore microbiota dynamics and drivers of  
463 susceptibility to RTIs. Strengths of our study include the frequency of sampling and the  
464 consistency in data and sample collection by trained doctors and research nurses. We made a

465 rigorous effort to minimize the potential effect of environmental contamination on low-density  
466 nasopharyngeal samples collected from children at very early age. Last, we used non-  
467 parametric, machine-learning techniques combined with (multivariable) spline-based mixed  
468 models to explore specific age-dependent patterns in microbial succession.

469 Our study also has limitations. First, parents were asked to contact the research team in  
470 case of a RTI. Therefore, likely not all RTI episodes may have been captured for in depth  
471 analyses. Exhaustive efforts were however made to obtain detailed information on all  
472 experienced RTIs when questionnaires were filled out during regular home visits to minimize  
473 reporting bias in our multivariable analyses (Bosch *et al*, unpublished data). Second, despite  
474 frequent sampling, our samples capture snapshots of a highly dynamic and developing  
475 microbiome, therefore we can only make assumptions about the dynamics in between sampling  
476 moments. Third, although we observed that microbiota changes seem to forego RTIs and are  
477 associated with RTI susceptibility, our study design precludes any definite statements on  
478 causality.

479 We here provide evidence that accelerated microbiota maturation is associated with  
480 microbiota instability and number of RTIs over the first year of life. These changed dynamics  
481 could be observed as early as within the first month of age, i.e. prior to the first RTI experiences.  
482 We also were able to link the impact of known important drivers such birth mode, feeding type,  
483 the presence of siblings, early day-care attendance, and recent use of antimicrobial therapy, via  
484 altered microbiota development to susceptibility to RTIs. The potential implications of these  
485 findings for our understanding of pathogenesis of disease, as well as diagnostic and preventive  
486 strategies, deserves further investigation.

487

488 **Acknowledgments**

489 We gratefully acknowledge the department of Obstetrics and Gynecology of the Spaarne  
490 Gasthuis and participating midwifery clinics for recruiting participants for this study; the  
491 research team of the Spaarne Gasthuis Academy for their execution of and dedication to the  
492 study; the laboratory staff of the University Medical Center Utrecht and TNO for their lab work  
493 and the cooperating institutes for their commitment to the project. Most of all, we are indebted  
494 to all the participating children and their families.

495

496 **Competing interests**

497 No conflict of interest related to the present study. EAMS declares to have received unrestricted  
498 research support from Pfizer, grant support for vaccine studies from Pfizer and GSK and fees  
499 paid to the institution for advisory boards or participation in independent data monitoring  
500 committees for Pfizer and GSK. No other authors reported financial disclosures. Funding  
501 sources had no role in the study design, in the collection, analysis and interpretation of data, in  
502 writing the report, and the decision to submit the paper for publication. The corresponding  
503 author had full access to all the data in the study and had final responsibility for the decision to  
504 submit for publication.

505

506

507



508 **References**

- 509 1. Liu L, Oza S, Hogan D, Chu Y, Perin J, Zhu J, Lawn JE, Cousens S, Mathers C, Black  
510 RE. Global, regional, and national causes of under-5 mortality in 2000-15: an updated  
511 systematic analysis with implications for the Sustainable Development Goals. *Lancet*  
512 2016;388:3027–3035.
- 513 2. Global Burden of Disease Study 2013 Collaborators. Global, regional, and national  
514 incidence, prevalence, and years lived with disability for 301 acute and chronic  
515 diseases and injuries in 188 countries, 1990-2013: a systematic analysis for the Global  
516 Burden of Disease Study 2013. *Lancet* 2015;386:743–800.
- 517 3. Donnelly JP, Baddley JW, Wang HE. Antibiotic utilization for acute respiratory tract  
518 infections in U.S. emergency departments. *Antimicrob Agents Chemother*  
519 2014;58:1451–1457.
- 520 4. Bosch AATM, Levin E, van Houten MA, Hasrat R, Kalkman G, Biesbroek G, de  
521 Steenhuijsen Piters WAA, de Groot P-KCM, Pernet P, Keijser BJF, Sanders EAM,  
522 Bogaert D. Development of Upper Respiratory Tract Microbiota in Infancy is Affected  
523 by Mode of Delivery. *EBioMedicine* 2016;9:336–345.
- 524 5. Chu DM, Ma J, Prince AL, Antony KM, Seferovic MD, Aagaard KM. Maturation of  
525 the infant microbiome community structure and function across multiple body sites and  
526 in relation to mode of delivery. *Nat Med* 2017;23:314–326.
- 527 6. Bokulich NA, Chung J, Battaglia T, Henderson N, Jay M, Li H, D Lieber A, Wu F,  
528 Perez-Perez GI, Chen Y, Schweizer W, Zheng X, Contreras M, Dominguez-Bello MG,  
529 Blaser MJ. Antibiotics, birth mode, and diet shape microbiome maturation during early  
530 life. *Sci Transl Med* 2016;8:343ra82–343ra82.
- 531 7. Bogaert D, Keijser B, Huse S, Rossen J, Veenhoven R, van Gils E, Bruin J, Montijn R,  
532 Bonten M, Sanders E. Variability and diversity of nasopharyngeal microbiota in  
533 children: a metagenomic analysis. *PLoS ONE* 2011;6:e17035.
- 534 8. Biesbroek G, Bosch AATM, Wang X, Keijser BJF, Veenhoven RH, Sanders EAM,  
535 Bogaert D. The Impact of Breastfeeding on Nasopharyngeal Microbial Communities in  
536 Infants. *Am J Respir Crit Care Med* 2014;190:298–308.
- 537 9. Blaser MJ. Antibiotic use and its consequences for the normal microbiome. *Science*  
538 2016;352:544–545.
- 539 10. Biesbroek G, Tsvitshivadze E, Sanders EAM, Montijn R, Veenhoven RH, Keijser BJF,  
540 Bogaert D. Early respiratory microbiota composition determines bacterial succession  
541 patterns and respiratory health in children. *Am J Respir Crit Care Med* 2014;190:1283–  
542 1292.
- 543 11. Vissing NH, Chawes BLK, Bisgaard H. Increased risk of pneumonia and bronchiolitis  
544 after bacterial colonization of the airways as neonates. *Am J Respir Crit Care Med*  
545 2013;188:1246–1252.
- 546 12. Gollwitzer ES, Saglani S, Trompette A, Yadava K, Sherburn R, McCoy KD, Nicod LP,  
547 Lloyd CM, Marsland BJ. Lung microbiota promotes tolerance to allergens in neonates  
548 via PD-L1. *Nat Med* 2014;20:642–647.
- 549 13. Olszak T, An D, Zeissig S, Vera MP, Richter J, Franke A, Glickman JN, Siebert R,  
550 Baron RM, Kasper DL, Blumberg RS. Microbial exposure during early life has  
551 persistent effects on natural killer T cell function. *Science* 2012;336:489–493.
- 552 14. Hooper LV, Littman DR, Macpherson AJ. Interactions between the microbiota and the  
553 immune system. *Science* 2012;336:1268–1273.
- 554 15. Kamada N, Chen GY, Inohara N, Núñez G. Control of pathogens and pathobionts by  
555 the gut microbiota. *Nat Immunol* 2013;14:685–690.
- 556 16. Man WH, de Steenhuijsen Piters WAA, Bogaert D. The microbiota of the respiratory  
557 tract: gatekeeper to respiratory health. *Nat Rev Microbiol* 2017;8:51.

- 558 17. Pettigrew MM, Laufer AS, Gent JF, Kong Y, Fennie KP, Metlay JP. Upper respiratory  
559 tract microbial communities, acute otitis media pathogens, and antibiotic use in healthy  
560 and sick children. *Appl Environ Microbiol* 2012;78:6262–6270.
- 561 18. Hilty M, Qi W, Brugger SD, Frei L, Agyeman P, Frey PM, Aebi S, Muhlemann K.  
562 Nasopharyngeal microbiota in infants with acute otitis media. *J Infect Dis*  
563 2012;205:1048–1055.
- 564 19. de Steenhuijsen Piters WAA, Heinonen S, Hasrat R, Bunsow E, Smith B, Suarez-  
565 Arrabal M-C, Chaussabel D, Cohen DM, Sanders EAM, Ramilo O, Bogaert D, Mejias  
566 A. Nasopharyngeal Microbiota, Host Transcriptome, and Disease Severity in Children  
567 with Respiratory Syncytial Virus Infection. *Am J Respir Crit Care Med*  
568 2016;194:1104–1115.
- 569 20. Teo SM, Mok D, Pham K, Kusel M, Serralha M, Troy N, Holt BJ, Hales BJ, Walker  
570 ML, Hollams E, Bochkov YA, Grindle K, Johnston SL, Gern JE, Sly PD, Holt PG,  
571 Holt KE, Inouye M. The infant nasopharyngeal microbiome impacts severity of lower  
572 respiratory infection and risk of asthma development. *Cell Host and Microbe*  
573 2015;17:704–715.
- 574 21. de Steenhuijsen Piters WAA, Sanders EAM, Bogaert D. The role of the local microbial  
575 ecosystem in respiratory health and disease. *Philosophical Transactions of the Royal*  
576 *Society B: Biological Sciences* 2015;370:20140294.
- 577 22. O'Brien KL, Nohynek H, World Health Organization Pneumococcal Vaccine Trials  
578 Carriage Working Group. Report from a WHO working group: standard method for  
579 detecting upper respiratory carriage of *Streptococcus pneumoniae*. *Pediatr Infect Dis J*  
580 2003;22:133–140.
- 581 23. Wyllie AL, Chu MLJN, Schellens MHB, van Engelsdorp Gastelaars J, Jansen MD, van  
582 der Ende A, Bogaert D, Sanders EAM, Trzciński K. *Streptococcus pneumoniae* in  
583 Saliva of Dutch Primary School Children. *PLoS ONE* 2014;9:e102045.
- 584 24. Subramanian S, Huq S, Yatsunenkov T, Haque R, Mahfuz M, Alam MA, Benezra A,  
585 DeStefano J, Meier MF, Muegge BD, Barratt MJ, VanArendonk LG, Zhang Q,  
586 Province MA, Petri WA, Ahmed T, Gordon JI. Persistent gut microbiota immaturity in  
587 malnourished Bangladeshi children. *Nature* 2014;510:417–421.
- 588 25. Dominguez-Bello MG, Costello EK, Contreras M, Magris M, Hidalgo G, Fierer N,  
589 Knight R. Delivery mode shapes the acquisition and structure of the initial microbiota  
590 across multiple body habitats in newborns. *Proc Natl Acad Sci USA* 2010;107:11971–  
591 11975.
- 592 26. Laufer AS, Metlay JP, Gent JF, Fennie KP, Kong Y, Pettigrew MM. Microbial  
593 communities of the upper respiratory tract and otitis media in children. *mBio*  
594 2011;2:e00245–10.
- 595 27. Hunt KM, Foster JA, Forney LJ, Schütte UM, Beck DL, Abdo Z, Fox LK, Williams  
596 JE, McGuire MK, McGuire MA. Characterization of the diversity and temporal  
597 stability of bacterial communities in human milk. *PLoS ONE* 2011;6:e21313.
- 598 28. Bomar L, Brugger SD, Yost BH, Davies SS, Lemon KP. *Corynebacterium accolens*  
599 Releases Antipneumococcal Free Fatty Acids from Human Nostril and Skin Surface  
600 Triacylglycerols. *mBio* 2016;7:.
- 601 29. Prevaes SMPJ, de Winter-de Groot KM, Janssens HM, de Steenhuijsen Piters WAA,  
602 Tramper-Stranders GA, Wyllie AL, Hasrat R, Tiddens HA, van Westreenen M, van der  
603 Ent CK, Sanders EAM, Bogaert D. Development of the Nasopharyngeal Microbiota in  
604 Infants with Cystic Fibrosis. *Am J Respir Crit Care Med* 2016;193:504–515.
- 605 30. Holgerson PL, Vestman NR, Claesson R, Ohman C, Domellöf M, Tanner ACR,  
606 Hernell O, Johansson I. Oral microbial profile discriminates breast-fed from formula-  
607 fed infants. *J Pediatr Gastroenterol Nutr* 2013;56:127–136.

- 608 31. Følsgaard NV, Schjørring S, Chawes BL, Rasmussen MA, Krogfelt KA, Brix S,  
609 Bisgaard H. Pathogenic bacteria colonizing the airways in asymptomatic neonates  
610 stimulates topical inflammatory mediator release. *Am J Respir Crit Care Med*  
611 2013;187:589–595.
- 612 32. Clarke KR. Non-parametric multivariate analyses of changes in community structure.  
613 *Australian journal of ecology* 1993;doi:10.1111/j.1442-9993.1993.tb00438.x/full.  
614  
615

616 **Figure legends**

617 **Figure 1** – Microbiota development over the first year of life.

618 **(A)** Relative abundance of the 15 highest ranking OTUs over the first year of life (age in days)  
619 and during of RTIs. OTUs are colour coded as indicated in the figure legend, which was based  
620 on their phylum level taxonomic annotation: red, Firmicutes; yellow, Actinobacteria; blue,  
621 Proteobacteria and green, Bacteroidetes. We observed a high abundance of Firmicutes  
622 (*Staphylococcus* (3) and *Dolosigranulum* (4)) and Actinobacteria (*Corynebacterium* spp.) early  
623 in life, which was gradually replaced by Proteobacteria (*Moraxella* (1), *Moraxella* (7),  
624 *Haemophilus* (6) and *Neisseria* spp.). OTUs that were not among the 15 highest ranking were  
625 collapsed and referred to as ‘Residuals’, stratified by phylum for the five most abundant phyla.

626 **(B)** Relative abundance of the 15 highest ranking OTUs over the first two months of life.  
627 Visualisation of microbiota profiles per time point allows for a more detailed assessment of  
628 microbial dynamics at early time points. Over the first week of life, a relatively high abundance  
629 of *Streptococcus* (5), *Janthinobacterium* (13) and *Neisseria* spp. and *Rothia* (12) was observed,  
630 apart from other OTUs belonging mainly to the Firmicutes, Proteobacteria and Actinobacteria  
631 phyla (See Figure E5). d = day; w = week; m = month.

632 **Figure 2** – Non-metric multidimensional scaling (nMDS) plot visualizing the microbiota  
633 succession patterns in the first year of life.

634 Each point represents the microbial community composition of one sample. Samples taken  
635 during health (n=1,065) are coloured based on the age at which they were taken (colours  
636 ranging from yellow [day 0] to dark green [year 1]). In addition, samples taken during RTI are  
637 depicted (n=56; dark red). The standard deviation of data points within time point/RTI strata is  
638 shown by ellipses. The 15 highest ranked OTUs were simultaneously visualized (triangles).

639 The size of the triangles is relative to the mean relative abundance of the OTU it represents.  
640 The stress value indicates how well the high-dimensional data are captured in the two-  
641 dimensional space; a value of ~0.2 indicates that the representation of some points is potentially  
642 misleading and that a representation in a higher dimensional space might be more appropriate  
643 (see Figure E4 for detailed assessment) (32). d = day; w = week; m = month; RTI = respiratory  
644 tract infection.

645 **Figure 3** – Absolute bacterial density over the first year of life.

646 Boxplots showing the absolute bacterial density (in pg/ $\mu$ L 16S-rRNA-gene) in blanks (n=55;  
647 blue), in samples taken during health at various time points (n=1,065; colours ranging from  
648 yellow [day 0] to dark green [year 1]) and during RTI (n=56; red). Bacterial density is  
649 particularly low at days 0 and 1, then gradually increases until the age of ~1 month, after which  
650 it remained largely stable. Box plots represent the 25<sup>th</sup> and 75<sup>th</sup> percentiles (lower and upper  
651 boundaries boxes, respectively), the median (middle horizontal line), and measurements that  
652 fall within 1.5 times the interquartile range (IQR; distance between 25<sup>th</sup> and 75<sup>th</sup> percentiles;  
653 whiskers) or outside 1.5 times the IQR (points). Q-values were derived from a linear mixed  
654 model with log<sub>10</sub>-transformed bacterial density as outcome variable, time point as fixed effect  
655 and subject as a random effect. Only samples taken at regular intervals were considered and  
656 each consecutive time point was compared to the previous time point using the *multcomp*  
657 package. \*\*\*, q-value <0.001; \*\*, 0.001  $\leq$  q-value <0.01. d = day; w = week; m = month; RTI  
658 = respiratory tract infection.

659 **Figure 4** – Microbiota maturation and age-discriminatory taxa stratified by RTI susceptibility.

660 **(A)** Microbiota age estimates plotted against chronological age stratified by number of RTIs  
661 experienced during the first year of life. The curves represent smooth spline fits for each cohort.

662 P-values are based on a linear mixed model, including age (spline) and number of RTIs (i.e. 0-  
663 2, 3-4 or 5-7 RTIs) as fixed effects and subject as random effect.

664 **(B)** Heatmap of the mean relative abundance of the 22 age-discriminatory OTUs against  
665 moment of sampling in each cohort. OTUs are ordered vertically based on average linkage  
666 hierarchical clustering using the Euclidean distance matrix. Colours correspond with row wise  
667 normalized relative abundances (i.e. red indicates the maximum relative abundance of that OTU  
668 over all cohorts, black indicates the minimum relative abundance). OTU-names are bold and  
669 coloured green if they were significantly enriched in the reference group (0-2 RTIs) compared  
670 to children with >2 RTIs. Red was used to denote the OTUs that were observed in higher  
671 abundance in children with >2 RTIs (based on SS-ANOVA q-values; see Table 4A). d = day;  
672 w = week; m = month; RTI = respiratory tract infection.

673 **(C)** Relative microbiota age (RMA) before (light green shades), during (red) and after RTI  
674 (dark green). The relative microbiota age two time points before RTI ('-2'; n=51; on average -  
675 104 days to RTI), one time point before RTI ('-1'; n=47; -50 days to RTI), at RTI ('RTI'; n=56;  
676 mean age at sampling of 216 days) and after RTI ('+1'; n=41; +57 days after RTI) is depicted  
677 in boxplots (see legend Figure 2). RMA already increased at time points preceding a factual  
678 RTI (median RMA +7.3 days at T = -2, +37.1 days at T = -1, and +67.8 days at RTI). P-values  
679 are based on a linear mixed model including timing of sampling (i.e. '-2', '-1', 'RTI' or '+1')  
680 and age (continuous) as fixed effects and subject as random effect. The contrasts '-2' vs '-1', '-  
681 1 vs 'RTI' and 'RTI' vs '+1' were tested (*multcomp* package). \*\*,  $0.001 \leq q\text{-value} < 0.01$ ; \*,  
682  $0.01 \leq q\text{-value} < 0.05$ .

683 **Figure 5** – Microbiota stability over time stratified by RTI susceptibility.

684 Bray-Curtis dissimilarities were calculated within each subject between each pair of

685 consecutive time points. The bacterial community stability was significantly lower in children  
686 with 3-4 ( $p=0.005$ ) or 5-7 RTIs ( $p=0.02$ ) compared to the reference group of children  
687 experiencing 0-2 RTIs within the first year of life. P-values are based on a linear mixed model,  
688 including age (spline) and number of RTIs as fixed effects and subject as random effect. The  
689 shaded area around each smoothing spline represents the 95% confidence interval.

690

691 **Legends Online Supplement**

692

693 **Methods** – Online supplement methods.

694

695 **Figure E1** – Flow chart study.

696 Flow chart showing the number of initially enrolled women and the reasons for exclusion of  
697 participants.

698 **Figure E2** – Distribution of respiratory tract infections within the cohort.

699 Histogram of the number of RTIs versus their frequency. ‘*N*’ denotes the number of individuals,  
700 ‘*n*’ gives the number of samples. The cohort was divided in RTI groups based on the distribution  
701 of RTIs; each sub cohort corresponds with a tertile.

702 **Figure E3** – OTU selection procedure.

703 **(A)** Plot showing the 10-fold cross-validation error (mean  $\pm$  standard deviation) as a function of  
704 the number of OTUs used to regress against chronological age in the reference cohort (children  
705 with 0-2 RTIs). An optimal trade-off between the mean squared error (MSE; i.e. cross-  
706 validation error) and number of OTUs in the model was observed at 22 OTUs.

707 **(B)** Age-discriminatory OTUs ranked in descending order based on their importance to the  
708 accuracy of the model. OTU importance was estimated by calculating the increase in mean-  
709 squared error (MSE) of the microbiota age prediction after randomly permuting the relative  
710 abundance values of each given OTU (mean  $\pm$  standard deviation, 100 replicates).

711 **Figure E4** – nMDS diagnostic plots and three-dimensional nMDS.



712 **(A)** Scree plot to depict the relationship between the number of (nMDS)-dimensions and stress.  
713 Naturally, the stress will reduce by increasing the number of dimensions, however only a  
714 maximum number of three dimensions can reasonably be interpreted. Using three dimensions  
715 the stress-value drops well below 0.2 (32), suggesting that a decent ordination of the data is  
716 possible in this number of dimensions.

717 **(B)** Three-dimensional nMDS plot. The main data structure visualized using the two-  
718 dimensional plot appears to be preserved when plotting the same data in three dimensions.

719 **Figure E5** – Relative abundance of early colonizing bacteria.

720 Bar plots visualizing the relative abundance (mean  $\pm$  standard error of the mean) of the 10  
721 highest ranking OTUs at each (early) time point (only considering day 0 and 1 and week 1 and  
722 2). For each OTU, we calculated the significance of change in relative abundance for each pair  
723 of consecutive time points (i.e. day 0 vs day 1, day 1 vs week 1 and week 1 vs week 2) using  
724 mixed linear models including subject as random effect. Significant differences between  
725 contrasts were determined using the *multcomp*-package. A Benjamini-Hochberg procedure was  
726 used to correct for multiple comparisons (simultaneously considering all OTUs/contrasts). \*\*\*,  
727 q-value <0.001; \*\*, 0.001  $\leq$  q-value <0.01; \*, 0.01  $\leq$  q-value <0.05.

728 **Figure E6** – Individual microbial developmental trajectories in time.

729 Using average linkage hierarchical clustering based on the Bray-Curtis dissimilarity matrix  
730 samples were binned into 8 clusters consisting of  $\geq 10$  samples. These clusters were enriched  
731 for *Moraxella* (1) (MOR1) *Corynebacterium* (2) and *Dolosigranulum* (4) (CDG),  
732 *Staphylococcus* (3) (STA) and *Streptococcus* (5) (STR), *Moraxella* (7) (MOR7), *Haemophilus*  
733 (6) (HAE), *Corynebacterium* (8) (COR8) and *Neisseria* spp. (NEI). The number of individuals  
734 in each cluster at each time point was visualised in alluvial diagrams, which were stratified by

735 the number of RTIs experienced over the first year of life (i.e. (A) 0-2 RTIs, (B) 3-4 RTIs and  
736 (C) 5-7 RTIs). The height of the figures corresponds with the total number of samples within  
737 that group. In addition, the height of the nodes and the thickness of the lines connecting the  
738 nodes is proportional to the number of samples. We observed that the CDG-cluster is  
739 underrepresented in children who experienced 5-7 RTIs over time. Instead, the early-life STA-  
740 cluster rapidly transitions into the MOR1-cluster, which is associated with older ages.

741 **Figure E7** – Relative abundance of age-discriminatory taxa at each time point. The line plots  
742 indicate the microbiota development for each age-discriminatory taxum. Dots represent mean  
743 relative abundance at a given time point within the stratum and whiskers depict the standard  
744 error of the mean. See Table E4 for statistical assessment. d = day; w = week; m = month.

745 **Figure E8** – Relative microbiota age stratified by time point and RTI cohort.

746 Boxplots (see legend Figure 3) depicting relative microbiota age (RMA) for each cohort. The  
747 RMA was significantly higher in children who experienced 5-7 RTIs compared to the reference  
748 group, after adjusting for either age or sampling moment (both  $p=0.007$ ).

749 **Figure E9** – Relative abundance of age-discriminatory taxa before (light green shades), during  
750 (red) and after RTI (dark green; see also legend figure 4C). Relative abundances were depicted  
751 using boxplots (see legend Figure 3). We tested the statistical significance of differences in  
752 microbial abundance between sampling moments using a linear mixed model including timing  
753 of sampling (i.e. ‘-2’, ‘-1’, ‘RTI’ or ‘+1’) and age (continuous) as fixed effects and subject as  
754 random effect. The contrasts ‘-2’ vs ‘-1’, ‘-1 vs ‘RTI’ and ‘RTI’ vs ‘+1’ were tested (*multcomp*  
755 package). Although we did observe changes in abundance of individual OTUs that appeared to  
756 be related to changes in RMA, these changes were not statistically significant (after adjusting  
757 for multiple testing).

758 **Figure E10** –  $\alpha$ -diversity measures stratified by RTI susceptibility.

759 We tested the number of observed species, Simpson and Shannon diversity indices. No  
760 significant differences between RTI groups were observed. Points represent mean values and  
761 whiskers depict the standard error of the mean. P-values were derived from mixed linear models  
762 with subject as random effect and adjusted for age (spline);  $p > 0.05$ ). d = day; w = week; m =  
763 month.

764 **Figure E11** – Relative abundance of the 15 highest ranking OTUs during the first year of life  
765 stratified by birth mode and feeding type - flow diagram.

766 See legend Figure 1A. We observed an increased relative abundance of *Corynebacterium* (2)  
767 and *Dolosigranulum* (4) until the age of five months and late *Moraxella* spp. enrichment in  
768 children vaginally delivered and/or breastfed. Birth by caesarean section was associated with  
769 early *Staphylococcus* (3) predominance. Feeding type was studied as a categorical variable  
770 indicating whether children were exclusively breastfed (BF) up to the age of three months (3m).  
771 See Table E6 and E7 for statistical assessment.

772 **Figure E12** – Relative abundance of the 15 highest ranking OTUs during the first year of life  
773 stratified by birth mode and feeding type - line plots.

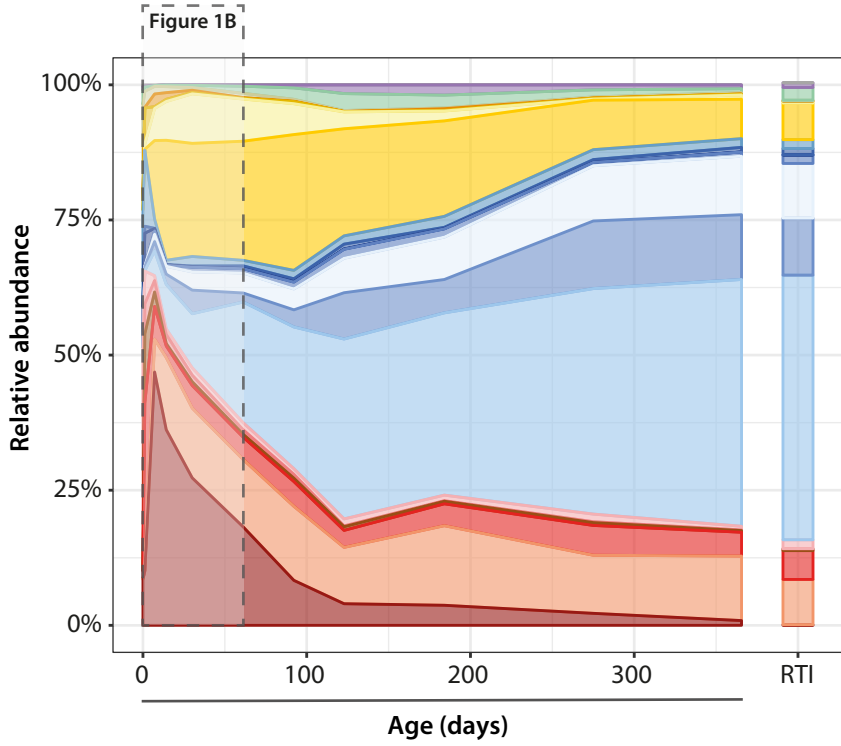
774 **(A)** Line plots indicating the microbiota succession patterns of abundant taxa, stratified by birth  
775 mode (caesarean section vs vaginal). Points represent means and whiskers represent standard  
776 errors of the mean. See Table E6 for statistical assessment. d = day; w = week; m = month; RTI  
777 = respiratory tract infection.

778 **(B)** Line plots indicating the microbiota succession patterns of abundant taxa, stratified by  
779 feeding type (exclusive breastfeeding up to the age of three months yes/no). Points represent

780 means and whiskers represent standard errors of the mean. See Table E10 for statistical  
781 assessment. d = day; w = week; m = month; RTI = respiratory tract infection.

**Figure 1**

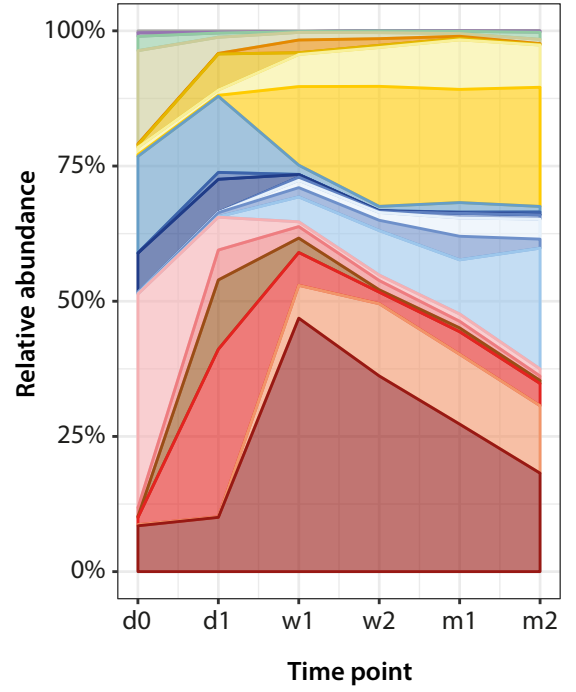
**A**



- Firmicutes**
- *Staphylococcus* (3)
  - *Dolosigranulum* (4)
  - *Streptococcus* (5)
  - *Gemella* (9)
  - *Streptococcus* (10)
  - Residuals Firmicutes

- Proteobacteria**
- *Moraxella* (1)
  - *Haemophilus* (6)
  - *Moraxella* (7)
  - *Neisseria* (11)
  - *Janthinobacterium* (13)
  - *Neisseria* (14)
  - Residuals Proteobacteria

**B**



- Actinobacteria**
- *Corynebacterium* (2)
  - *Corynebacterium* (8)
  - *Rothia* (12)
  - *Corynebacterium* (15)
  - Residuals Actinobacteria
  - Residuals Bacteroidetes
  - Residuals Fusobacteria
  - Residuals

Figure 2

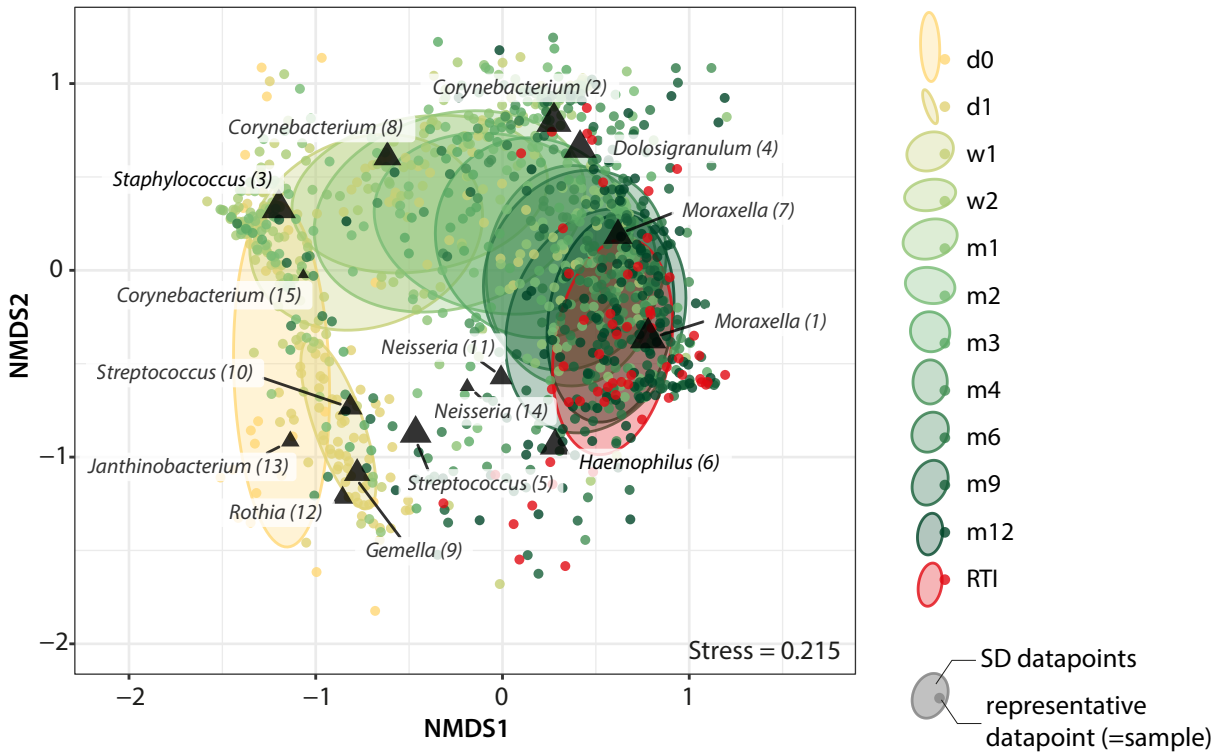


Figure 3

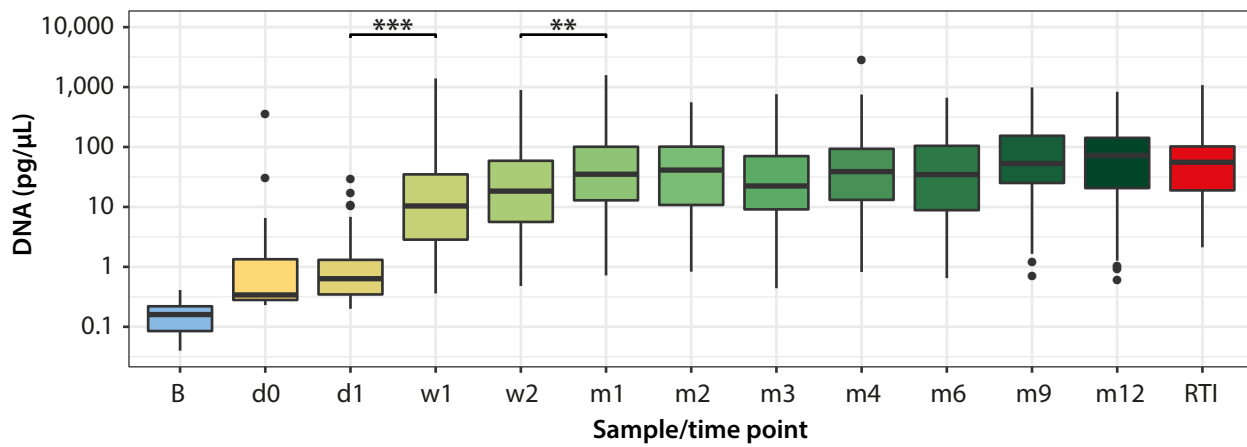
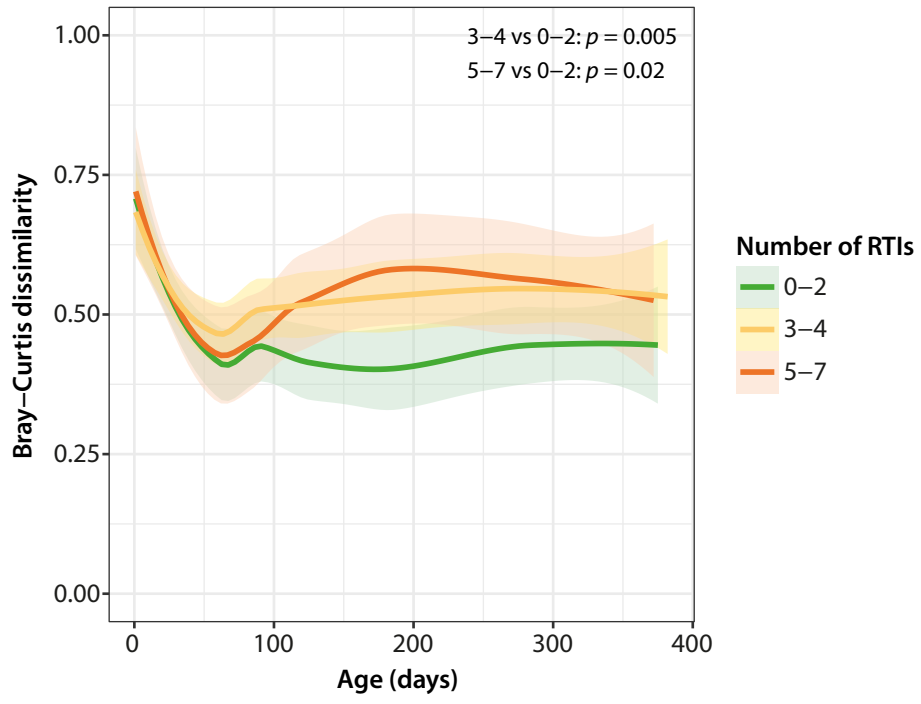






Figure 5



1 **ONLINE SUPPLEMENT**

2

3 **Title:** Maturation of the infant respiratory microbiota, environmental drivers and health  
4 consequences: a prospective cohort study

5

6 **Authors:** Astrid A.T.M. Bosch<sup>†</sup>, Wouter A.A. de Steenhuijsen Pipers<sup>†</sup>, Marlies A. van Houten,  
7 Mei Ling J.N. Chu, Giske Biesbroek, Jolanda Kool, Paula Pernet, Pieter-Kees C.M. de Groot,  
8 Marinus J.C. Eijkemans, Bart J.F. Keijser, Elisabeth A.M. Sanders and Debby Bogaert\*

9

10 <sup>†</sup> These authors contributed equally to this work

11 \* Corresponding author. Email: D.Bogaert@ed.ac.uk.

12

13 **This file includes:**

14 (Online supplement) Methods

15

16 **Other supplementary materials for this manuscript include the following:**

17 Figures E1-E12, as a separate pdf-file.

18 Tables E1-E7, including captions, as a separate excel spreadsheet.

19

20

21 **Methods**

22 *Study population*

23 Nasopharyngeal swabs were collected from healthy children who participated in an ongoing  
24 prospective birth cohort study. The primary aim of this population-based study is to investigate  
25 the development and dynamics of the microbiota in infants during health and disease, with  
26 special interest in the impact of mode of delivery on microbial succession. Since approximately  
27 15% of the Dutch children are born by caesarian section (E1), the cohort is enriched by  
28 caesarian section deliveries with the aim to obtain a ~50/50 distribution between caesarian  
29 section born children and vaginally delivered children. The study is conducted in the  
30 Netherlands, a small country (approximately 17 million inhabitants) in North-Europe with high  
31 socio-economic standards and a moderate sea climate characterized by cool summers and mild  
32 winters.

33

34 The trials' methods have been described elsewhere (E2). In short, healthy, term born newborns  
35 (gestational age >37 weeks) were enrolled in the study directly after birth. Exclusion criteria at  
36 baseline were major congenital anomalies, severe maternal or neonatal complications during  
37 birth, language barrier, intention to move outside the research area, or parents under the age of  
38 18 years. Written informed consent was obtained from both parents before birth of the child.  
39 Participants did not receive any financial compensation. An acknowledged national Ethics  
40 Committee in the Netherlands (METC Noord-Holland, committee on research involving human  
41 subjects) approved the study (M012-015, NH012.394, NTR3986). The study was conducted in  
42 accordance with the European Statements for Good Clinical Practice. We estimated 10-20%  
43 loss to follow-up, therefore we had ethical approval to replace participants in case they dropped  
44 out of the study before six months of follow-up. Eventually we had complete datasets up to one

45 year of age of 116 participants. These infants were born between December 19<sup>th</sup>, 2012 and  
46 November 2<sup>st</sup>, 2014.

47 Of these 116 children, we had at least eight samples of good quality available for 112 children  
48 after laboratory work-up (Figure E1).

49

50 Our study was powered to detect differences in microbial communities between vaginally born  
51 children and children born by caesarian-section, which was the primary aim of the cohort study.

52 We performed power calculations aiming to be able to detect at least two-fold differences in at  
53 least the top 25 most common bacteria after correction for multiple testing. Given the variability  
54 and spread in abundance of OTUs we calculated that 40 children per group would give us  
55 sufficient power (>80%) to address our primary research question. Because the inclusion rate  
56 of caesarian-born children was lower than expected, we were allowed to extend the enrollment  
57 period, resulting in a much larger sample size (N=128) than initially expected, enabling us to  
58 thoroughly investigate secondary outcomes, such as the association between microbiota  
59 differences and the number of RTIs, again providing us with sufficient power to analyze group  
60 sizes of approximately 40 children per group.

61

## 62 *Data collection*

63 Home visits were conducted directly after birth, 24 hours after birth, at seven days, 14 days,  
64 and one, two, three, four, six, nine, and 12 of months of age. Postpartum visits were all  
65 performed within two hours from birth and all day one samples were obtained within 24-36  
66 hours after delivery. For logistic reasons (sampling preferably during office hours and  
67 considering parental vacations), we allowed some flexibility for the remaining sample  
68 moments: all week one samples were obtained within 5-9 days (mean 7); all week two samples  
69 between 12-17 days (mean 14); month one samples between 23-27 days (mean 30), months two

70 samples between 49-73 days (mean 61), months three samples between 83-111 days (mean 92),  
71 months four samples between 112-133 days (mean 123), months six between 177-197 days  
72 (mean 184), months nine samples between 260-288 (mean 275), months 12 samples between  
73 358-382 (mean 366) days postpartum, resulting in no overlap between sample moments (see  
74 Figure 4A).

75

76 Each home visit, nasopharyngeal samples were obtained by trained doctors and research nurses  
77 in a semi-sterile setting as previously described (E2). In short, deep nasopharyngeal swabs were  
78 collected trans nasally using a flexible, sterile swab (Copan eSwab, 484CE). Directly after  
79 sampling, the swabs were snap-frozen and stored in a sterile, filtered solution (10% Glycerol  
80 (VWR international BV 1.04093.1000) in 0.1% DEPC water (SERVA Electrophoresis,  
81 39798.03). The swabs were transported on dry ice and stored at -80°C until further analyses. In  
82 addition, the research team completed an extensive survey on the health status of the child and  
83 environmental factors, including breastfeeding, crowding conditions, and medication use.

84

85 Next to these regular and frequent visits, parents were asked to contact the study team in case  
86 of an active respiratory tract infections, defined as fever  $\geq 38^{\circ}\text{C}$  (per rectal measurement) for >6  
87 hours combined with general unwell feeling and presence of RTI symptoms, including earache,  
88 cough, hoarseness, wheeze, dyspnoea and/or runny nose. During an extra home visit (RTI visit  
89 within 48 hours after start of the fever), we collected additional nasopharyngeal samples using  
90 the same procedure as described above and obtained information about the duration of the fever,  
91 RTI symptoms, and antibiotic use. In addition, the research team called parents two to four  
92 weeks after the RTI visit to complete the questionnaire. Since 15 of the children had respiratory  
93 symptoms with fever during one of the regular visits, these were also considered as a RTI  
94 episode in the analyses.

95

96 *Bacterial DNA isolation and quantification*

97 Bacterial DNA from 200  $\mu$ l sample was isolated by bead-beating in phenol (E3) and quantified  
98 using a qPCR with primers directed at the 16S-rRNA gene (E4, 5). DNA was then eluted in  
99 two aliquots of 25  $\mu$ l elution buffer and stored at -20°C until further analyses.

100

101 *16S-rRNA gene amplicon sequencing*

102 PCR amplicon libraries were generated by amplification of the 16S ribosomal RNA gene using  
103 barcoded primers directed at the V4 hypervariable region, as previously described (E2). Primer  
104 pair 533F/806R was used for amplification. Amplicon pools from samples and controls were  
105 sequenced in eight runs using an Illumina MiSeq instrument, resulting in paired-end 200 or  
106 250 nucleotide reads. We first trimmed all reads to a length of 200 nucleotides (Fastx toolkit,  
107 version 0.0.13) and then applied an adaptive, window-based trimming algorithm (Sickle,  
108 version 1.33) (E6) using a quality threshold of Q30 and a length threshold of 150 nucleotides  
109 to filter out low quality reads/nucleotides. We aimed to further reduce the number of sequence  
110 errors in the reads by applying an error correction algorithm (BayesHammer, SPAdes genome  
111 assembler toolkit, version 3.5.0) (E7). After quality filtering and error correction, reads were  
112 assembled into contigs (PANDAseq, version 2.9) (E8, 9) and demultiplexed (Qiime version  
113 1.9.1; split\_libraries.py) (E10). We removed singleton sequences (1.4%) and identified  
114 chimeras using both *de novo* and reference chimera identification (UCHIME; 3.2%). After  
115 removal of chimeric sequences, VSEARCH abundance-based greedy clustering was used to  
116 pick OTUs at a 97% identity threshold (E11). OTUs were then annotated by the Naïve Bayesian  
117 RDP classifier (version 2.2) (E12) with a classification confidence of 50% (default) (E13) and  
118 annotations were based on the 97% identity SILVA 119 release reference database (E14). The  
119 SILVA-annotations for the most abundant/age-discriminatory taxa were verified using

120 BLASTN (E15) (Table E1). In the main text we further refer to OTUs using maximum genus  
121 level annotations, combined with a rank number based on the abundance of each given OTU.

122

### 123 *Data normalisation and filtering*

124 We generated an abundance-filtered dataset by including only those OTUs that were present at  
125 or above a confident level of detection (0.1% relative abundance) in at least two samples,  
126 retaining 576 OTUs (0.3% of reads excluded) (E16). We generated a rarefied OTU-table at a  
127 sequence depth of 3,500 reads, calculated the relative abundance of OTUs and used this table  
128 as input for downstream analyses, including visualisations, random forest modelling and  
129 stability analyses.  $\alpha$ -diversity measures were calculated for 100 rarefactions at a sequencing  
130 depth of 3500 reads and averaged. Raw read counts were normalised intrinsically using  
131 cumulative sum scaling (CSS) if modelling was performed using the *metagenomeSeq* package  
132 and the *fitTimeSeries* function (E17). Using this function, the temporal associations between  
133 each of the 22 age-discriminatory taxa and risk of RTIs were assessed; only significant results  
134 were reported. For the analyses on the temporal effects of birth mode and feeding type, OTUs  
135 with >10 sequences in  $\geq 50$  samples were included. Similarly, for analyses based on Multivariate  
136 Association with Linear Models (MaAsLin), we selected OTUs from the rarefied OTU-table  
137 with a relative abundance of >0.1% in  $\geq 50$  samples. Next, the OTU-table was expanded by  
138 calculating the cumulative relative abundance of the selected OTUs at all taxonomic levels (i.e.  
139 ranging from species/OTU-level to kingdom level).  $\beta$ -diversity was assessed using the Bray-Curtis  
140 dissimilarity metric.

141

### 142 *Quality control of 16S-rRNA gene amplicon sequencing*

143 URT samples, especially in very young children, are typically low in bacterial density (E18),  
144 and therefore measures to control for potential contamination with environmental DNA are

145 of vital importance. Since we were particularly interested in the initial colonization patterns of  
146 the children in our cohort, we set out to discern samples with a high likelihood of environmental  
147 contamination, from those samples that did not resemble negative DNA blanks through an  
148 unsupervised clustering approach. Both low DNA samples (0.2 pg/μl-0.5 pg/μl) and blanks  
149 (n=50; 30 excluded because of too low sequence depth) were rarefied to a depth of 2,000 reads  
150 and subjected to average linkage hierarchical clustering based on the Bray-Curtis dissimilarity  
151 (100 repeats). For each repeat, we used the maximum Silhouette index to determine the optimal  
152 number of clusters (up to 20 clusters tested). Samples that co-clustered with DNA blanks in  
153 >5% of the repeats were excluded from subsequent analyses, together with samples that were  
154 sequenced twice, samples with a density of <0.2 pg/μl or read counts <3,500 sequences, and  
155 samples of individuals that were lost to follow-up and/or had <8 samples available (in total 211  
156 samples excluded), resulting in 1,121 samples from 112 individuals. Sequence data of part of  
157 the samples (≤6 months) of part of the children (743 samples, 101 individuals) were used for a  
158 previous study on the role of mode of delivery on early respiratory microbiota development  
159 (E2).

160

161 In addition, we included 14 mock communities, consisting of 12 bacterial species commonly  
162 observed in the upper respiratory tract (i.e. *Bacteroides fragilis*, *Haemophilus influenzae*,  
163 *Streptococcus pneumoniae*, *Streptococcus pyogenes*, *Klebsiella oxytoca*, *Klebsiella*  
164 *pneumoniae*, haemolytic *Streptococcus* group A, *Pseudomonias aeruginosa*, *Staphylococcus*  
165 *epidermidis*, *Staphylococcus aureus* and *Moraxella catarrhalis*). Equivalent amounts of DNA  
166 isolated from these species were combined and included as internal controls in the Illumina  
167 MiSeq runs.

168

169 *Statistical analysis*



170 All analyses were performed in the R version 3.3.0 within R studio version 0.99.902. All figures  
171 were created using the *ggplot2* R-package and edited using Illustrator CC. We corrected for  
172 multiple testing if applicable using the Benjamini-Hochberg procedure (resulting in corrected  
173 P-values or q-values; *p.adjust* function). ‘Environmental factors’ used in the descriptions of the  
174 various models below comprises birth mode, breast feeding until three months of age, day care  
175 attendance, presence of siblings under five years of age, antibiotic treatment in the previous  
176 four weeks and season of birth, if not specified otherwise.

177

### 178 *Baseline tables*

179 Baseline tables were created using the *tableone* package (E19). Continuous variables were  
180 tested for normality using a Shapiro-Wilk test. Variables with a non-normal distribution were  
181 characterised using a median and interquartile range and the statistical significance of  
182 differences between groups was calculated using a Mann-Whitney U or Kruskal-Wallis test.  
183 Normally distributed variables were summarised by a mean and standard deviation and  
184 differences were tested for significance using a Student’s t-test/analysis of variance (ANOVA).  
185 For categorical variables, we used a Chi-square to test for statistically significant differences  
186 between groups. A Fisher’s exact test was used for categorical variables if the expected cell  
187 count was less than five.

188

### 189 *Non-metric multidimensional scaling and multivariate modelling*

190 Microbial succession patterns were visualised using non-metric multidimensional scaling  
191 (nMDS; *metaMDS* function in the *vegan* package; *trymax*=1,000) (E20) based on the Bray-  
192 Curtis dissimilarity matrix. Ellipses were calculated using the *veganCovEllipse* function and  
193 represent the standard deviation of data points. Stress-values, which indicate how well the  
194 ordination captured the high-dimensional data (i.e. a measure of goodness-of-fit), were

195 reported. We tested whether a nMDS-visualisation in a higher dimensional space would  
196 decrease the stress of the ordination using a scree plot (1-6 dimensions tested). Based on our  
197 findings (balancing number of dimensions, reduction in stress-value and interpretability of the  
198 plot) we decided to provide a three-dimensional nMDS plot as a supplementary figure.

199

200 To quantify the effect of environmental variables and number of RTIs on the overall microbiota  
201 composition we performed permutational multivariate analysis of variance (PERMANOVA)-  
202 tests (*adonis* function of the *vegan* package; Bray-Curtis dissimilarity, 999 permutations). To  
203 assess the robustness of our findings based on one rarefied OTU-table, we reran the same  
204 PERMANOVA-tests on 100 rarefied OTU-tables and compared the effect size of the variables  
205 under consideration across rarefactions (Table E3A and E3C).

206

### 207 *Clustering and alluvial diagram*

208 To complement our findings based on our group-level analyses, we additionally assessed  
209 microbial development at the individual level. We first clustered individuals using unsupervised  
210 average linkage hierarchical clustering based on the Bray-Curtis dissimilarity matrix. The  
211 number of clusters was determined based on the Silhouette and Calinski-Harabasz indices (*fpc*  
212 package) (E21). Clusters consisting  $\geq 10$  samples were considered for subsequent analyses. The  
213 proportion of samples within each cluster at each time point was visualised using an alluvial  
214 diagram (*ggvisSankey*-function within the *googleVis* package) (E22).

215 The alluvial diagram was stratified into three groups based on the normal distribution of RTIs  
216 in the population; 39 children with 0-2 RTIs (reference group), 52 children with 3-4 RTIs and  
217 21 children with 5-7 RTIs over the first year of life.

218

219 *Random forest modelling*

220 We hypothesized that the microbial succession patterns in the upper respiratory tract would be  
221 altered in children who are more susceptible to RTIs. To investigate this hypothesis, we used a  
222 machine learning technique referred to as random forest, which consists of an ensemble of  
223 decision trees, each of which is built based on random partition of the data, using a random  
224 selection of predictors (E23). We chose a random forest-approach over a more traditional,  
225 reductionist approach where we would model individual OTUs, as we did not want to make  
226 any assumptions on the highly variable relationships between specific OTUs and age (figure  
227 E7). Also, OTU-abundance data is usually very sparse and overdispersed, which hinders the  
228 application of traditional statistical techniques. Last, the random forest approach enabled us to  
229 simultaneously model these challenging data, as well as reduce the dimensionality of the data,  
230 the latter of which is essential to microbiota analysis.

231 To identify OTUs characteristic of a healthy microbiota maturation, we regressed the relative  
232 abundance of the 576 OTUs observed against chronological age in the reference group (i.e. 0-  
233 2 RTIs) using the *randomForest* package, (ntree=10,000, default mtry, defined as the number  
234 of variables in the model divided by 3) (E24), as previously described (E16). The optimal  
235 number of age-discriminatory taxa required for the prediction of microbiota age was determined  
236 by calculating the cross-validated prediction performance of models with a sequentially reduced  
237 numbers of variables (ranked by importance measured by the mean increase of squared error if  
238 that variable would be removed from the model; *caret* package (E25); 100 iterations; Figure  
239 E3A and E3B). This selection of OTUs was subsequently used as input to a random forest  
240 model used to regress the relative abundance versus chronological age in the reference group  
241 (resulting in the final model). We determined the importance of the reduced set of variables  
242 based on the percentage increase in mean squared error after permuting the values for each  
243 OTU (100 iterations). The final model was then used to predict chronological age, referred to

244 as ‘microbiota age’, in individuals who experienced 3-4 and 5-7 RTIs and on the group of  
245 samples collected during RTIs. We used the *train* function in the ‘caret’ package (E25) to  
246 determine cross-validated predictions of microbiota age for the healthy cohort (10 folds, 100  
247 iterations, default mtry) to avoid reporting overfitted estimates (Figure 4A). The importance of  
248 the age-discriminatory OTUs was visualised per cohort at each time point using a heatmap.  
249 OTUs were vertically ordered based on an average linkage hierarchical clustering to visualise  
250 the interrelations between OTUs. The colours of the heatmap were row-wise normalized (i.e.  
251 red indicates the highest relative abundance of that OTU, black indicates the lowest value.). As  
252 a post-hoc analysis, we studied the effect of the *Moraxella*-genus on the performance of the  
253 microbiota age model by excluding the OTUs belonging to the *Moraxella*-genus from the model  
254 while monitoring the amount of variance explained.

255  
256 Since the relationship between chronological age and microbiota age was not linear, we  
257 calculated the relative microbiota age as described before (E16). Relative microbiota age  
258 (RMA) was calculated as follows: relative microbiota age = microbiota age of a given child –  
259 microbiota age of children of similar age in the reference group (determined by a spline fit)  
260 (E16).

### 261 262 *Linear mixed models*

263 Linear mixed models were used to assess the effect of fixed variables on a continuous dependent  
264 variable, while including subject as a random intercept to adequately control for repeated  
265 measures (*lmer* function of the *lme4* package) (E26). Separate models were used study the effect  
266 of 1) environmental variables and 2) RTI susceptibility (defined as having experienced 0-2, 3-  
267 4 or 5-7 RTIs during the first year of life) on relative microbiota age, Bray-Curtis-dissimilarity  
268 and  $\alpha$ -diversity measures. If a non-linear relationship between age and the dependent variable

269 was suspected, age was included in the model as a natural spline fit with five degrees of freedom  
270 (*ns* function of the *splines* R-package). In addition, we assessed influence of sampling moment  
271 on bacterial density (log<sub>10</sub>-transformed) and relative abundance (only first four time points)  
272 using linear mixed models. Furthermore, we investigated the changes in RMA and the relative  
273 abundance of age-discriminatory taxa at two time points before RTI, during RTI and at one  
274 time point after RTI using a mixed linear model with RMA/OTU-abundance as outcome  
275 variables and including timing of sampling (i.e. '-2', '-1', 'RTI' or '+1'), age as fixed effects  
276 and subject as random effect. We did not consider interactions between variables in our models.  
277 Post-hoc tests on contrasts of interest were performed using the *multcomp* package (E27).  
278 Contrasts as specified in the main text were included and we adjusted for multiple testing using  
279 the 'single-step' procedure (*multcomp* default), except when stated otherwise.

280

### 281 *Time series modelling*

282 To assess differences in abundance of OTUs between groups, we used smoothing spline  
283 ANOVA as implemented in the *fitTimeSeries* function (E28) of the *metagenomeseq* R-package  
284 (E17), which aims to model the differences in OTU-abundances between groups over time and  
285 is able to not only test if differences exist, but also to evaluate the timing of these differences.  
286 In addition, this function allows for the inclusion of a 'class'-effect, to adequately control for  
287 repeated measures. Smoothing spline ANOVA models were used to study the (timing of)  
288 differential abundance of age-discriminatory taxa determined by random forest between  
289 children with 0-2 versus 3-4 RTIs and 0-2 versus 5-7 RTIs over the first year of life. In addition,  
290 these models were used to assess the effect of birth mode and exclusive breastfeeding until  
291 three months on the abundance of OTUs that passed the abundance filter, as these variables  
292 likely have a temporary effect on microbial abundance. P-values were determined based on  
293 1,000 permutations.

294

295 *Multivariable modelling*

296 To identify significant associations between environmental variables (as defined before) and  
297 the relative abundance of OTUs in a multivariable manner, we used Multivariate Association  
298 with Linear Models (MaAsLin). Age was included as a natural spline with five degrees of  
299 freedom. Taxonomic entities simultaneously included in the models were OTUs that passed the  
300 abundance filtering criterion and OTUs binned together at higher taxonomic levels (i.e. genus,  
301 family, class, order, phylum and kingdom). We included subject as a random effect and ran the  
302 models using default settings.

303

304 **References**

- 305 E1. Delnord M, Blondel B, Drewniak N, Klungsøyr K, Bolumar F, Mohangoo A, Gissler  
306 M, Szamotulska K, Lack N, Nijhuis J, Velebil P, Sakkeus L, Chalmers J, Zeitlin J,  
307 Euro-Peristat Preterm Group. Varying gestational age patterns in cesarean delivery:  
308 an international comparison. *BMC Pregnancy Childbirth* 2014;14:321.
- 309 E2. Bosch AATM, Levin E, van Houten MA, Hasrat R, Kalkman G, Biesbroek G, de  
310 Steenhuijsen Piters WAA, de Groot P-KCM, Pernet P, Keijser BJF, Sanders EAM,  
311 Bogaert D. Development of Upper Respiratory Tract Microbiota in Infancy is  
312 Affected by Mode of Delivery. *EBioMedicine* 2016;9:336–345.
- 313 E3. Wyllie AL, Chu MLJN, Schellens MHB, van Engelsdorp Gastelaars J, Jansen MD,  
314 van der Ende A, Bogaert D, Sanders EAM, Trzeciński K. Streptococcus pneumoniae  
315 in Saliva of Dutch Primary School Children. *PLoS ONE* 2014;9:e102045.
- 316 E4. Bogaert D, Keijser B, Huse S, Rossen J, Veenhoven R, van Gils E, Bruin J, Montijn  
317 R, Bonten M, Sanders E. Variability and diversity of nasopharyngeal microbiota in  
318 children: a metagenomic analysis. *PLoS ONE* 2011;6:e17035.
- 319 E5. Biesbroek G, Tsivtsivadze E, Sanders EAM, Montijn R, Veenhoven RH, Keijser BJF,  
320 Bogaert D. Early respiratory microbiota composition determines bacterial succession  
321 patterns and respiratory health in children. *Am J Respir Crit Care Med*  
322 2014;190:1283–1292.
- 323 E6. Joshi NA, Fass JN. Sickle: A sliding-window, adaptive, quality-based trimming tool  
324 for FastQ files. 1st ed. at <<https://github.com/najoshi/sickle>>.
- 325 E7. Nikolenko SI, Korobeynikov AI, Alekseyev MA. BayesHammer: Bayesian clustering  
326 for error correction in single-cell sequencing. *BMC Genomics* 2013;14 Suppl 1:S7.
- 327 E8. Masella AP, Bartram AK, Truszkowski JM, Brown DG, Neufeld JD. PANDAseq:  
328 paired-end assembler for illumina sequences. *BMC Bioinformatics* 2012;13:31.
- 329 E9. Schirmer M, Ijaz UZ, D'Amore R, Hall N, Sloan WT, Quince C. Insight into biases  
330 and sequencing errors for amplicon sequencing with the Illumina MiSeq platform.  
331 *Nucleic Acids Res* 2015;43:e37–e37.

- 332 E10. Caporaso JG, Kuczynski J, Stombaugh J, Bittinger K, Bushman FD, Costello EK,  
333 Fierer N, Peña AG, Goodrich JK, Gordon JI, Huttley GA, Kelley ST, Knights D,  
334 Koenig JE, Ley RE, Lozupone CA, McDonald D, Muegge BD, Pirrung M, Reeder J,  
335 Sevinsky JR, Turnbaugh PJ, Walters WA, Widmann J, Yatsunencko T, Zaneveld J,  
336 Knight R. QIIME allows analysis of high-throughput community sequencing data.  
337 *Nat Methods* 2010;7:335–336.
- 338 E11. Westcott SL, Schloss PD. De novo clustering methods outperform reference-based  
339 methods for assigning 16S rRNA gene sequences to operational taxonomic units.  
340 *PeerJ* 2015;3:e1487.
- 341 E12. Wang Q, Garrity GM, Tiedje JM, Cole JR. Naive Bayesian classifier for rapid  
342 assignment of rRNA sequences into the new bacterial taxonomy. *Appl Environ*  
343 *Microbiol* 2007;73:5261–5267.
- 344 E13. Claesson MJ, O'Sullivan O, Wang Q, Nikkilä J, Marchesi JR, Smidt H, de Vos WM,  
345 Ross RP, O'Toole PW. Comparative analysis of pyrosequencing and a phylogenetic  
346 microarray for exploring microbial community structures in the human distal  
347 intestine. *PLoS ONE* 2009;4:e6669.
- 348 E14. Quast C, Pruesse E, Yilmaz P, Gerken J, Schweer T, Yarza P, Peplies J, Glöckner  
349 FO. The SILVA ribosomal RNA gene database project: improved data processing  
350 and web-based tools. *Nucleic Acids Res* 2013;41:D590–6.
- 351 E15. Zhang Z, Schwartz S, Wagner L, Miller W. A greedy algorithm for aligning DNA  
352 sequences. *J Comput Biol* 2000;7:203–214.
- 353 E16. Subramanian S, Huq S, Yatsunencko T, Haque R, Mahfuz M, Alam MA, Benezra A,  
354 DeStefano J, Meier MF, Muegge BD, Barratt MJ, VanArendonk LG, Zhang Q,  
355 Province MA, Petri WA, Ahmed T, Gordon JI. Persistent gut microbiota immaturity  
356 in malnourished Bangladeshi children. *Nature* 2014;510:417–421.
- 357 E17. Paulson JN, Stine OC, Bravo HC, Pop M. Differential abundance analysis for  
358 microbial marker-gene surveys. *Nat Methods* 2013;10:1200–1202.
- 359 E18. Biesbroek G, Sanders EAM, Roeselers G, Wang X, Caspers MPM, Trzciński K,  
360 Bogaert D, Keijsers BJB. Deep sequencing analyses of low density microbial  
361 communities: working at the boundary of accurate microbiota detection. *PLoS ONE*  
362 2012;7:e32942.
- 363 E19. Yoshida K, Bohn J. tableone: Create “Table 1” to Describe Baseline Characteristics.  
364 0 ed. 2015;at <<https://CRAN.R-project.org/package=tableone>>.
- 365 E20. Oksanen J, Blanchet FG, Kindt R, Legendre P, Minchin PR, O'Hara RB, Simpson  
366 GL, Solymos P, Stevens M, Wagner H. vegan: Community Ecology Package. 2015;at  
367 <<http://CRAN.R-project.org/package=vegan>>.
- 368 E21. Hennig C. fpc: Flexible Procedures for Clustering. 2015;at <<http://CRAN.R-project.org/package=fpc>>.
- 370 E22. Gesmann M, de Castillo D. Using the Google Visualisation API with R. *R Journal*  
371 2011;3:40–44.
- 372 E23. Breiman L. Random forests. *Machine learning* 2001;
- 373 E24. Liaw A, Wiener M. Classification and Regression by randomForest. *R news*  
374 2002;2:18–22.
- 375 E25. Kuhn M. Building Predictive Models in R Using the caret Package. *J Stat Softw*  
376 2008;28:.
- 377 E26. Bates D, Mächler M, Bolker B, Walker S. Fitting Linear Mixed-Effects Models  
378 Using lme4. *J Stat Softw* 2015;67:.
- 379 E27. Hothorn T, Bretz F, Westfall P, Heiberger RM. Package “multcomp.” 2016;
- 380 E28. Talukder H, Paulson JN, Bravo HC. fitTimeSeries: Longitudinal differential  
381 abundance analysis for marker-gene surveys. *bioconductorjrp*

382  
383  
384



Figure E1

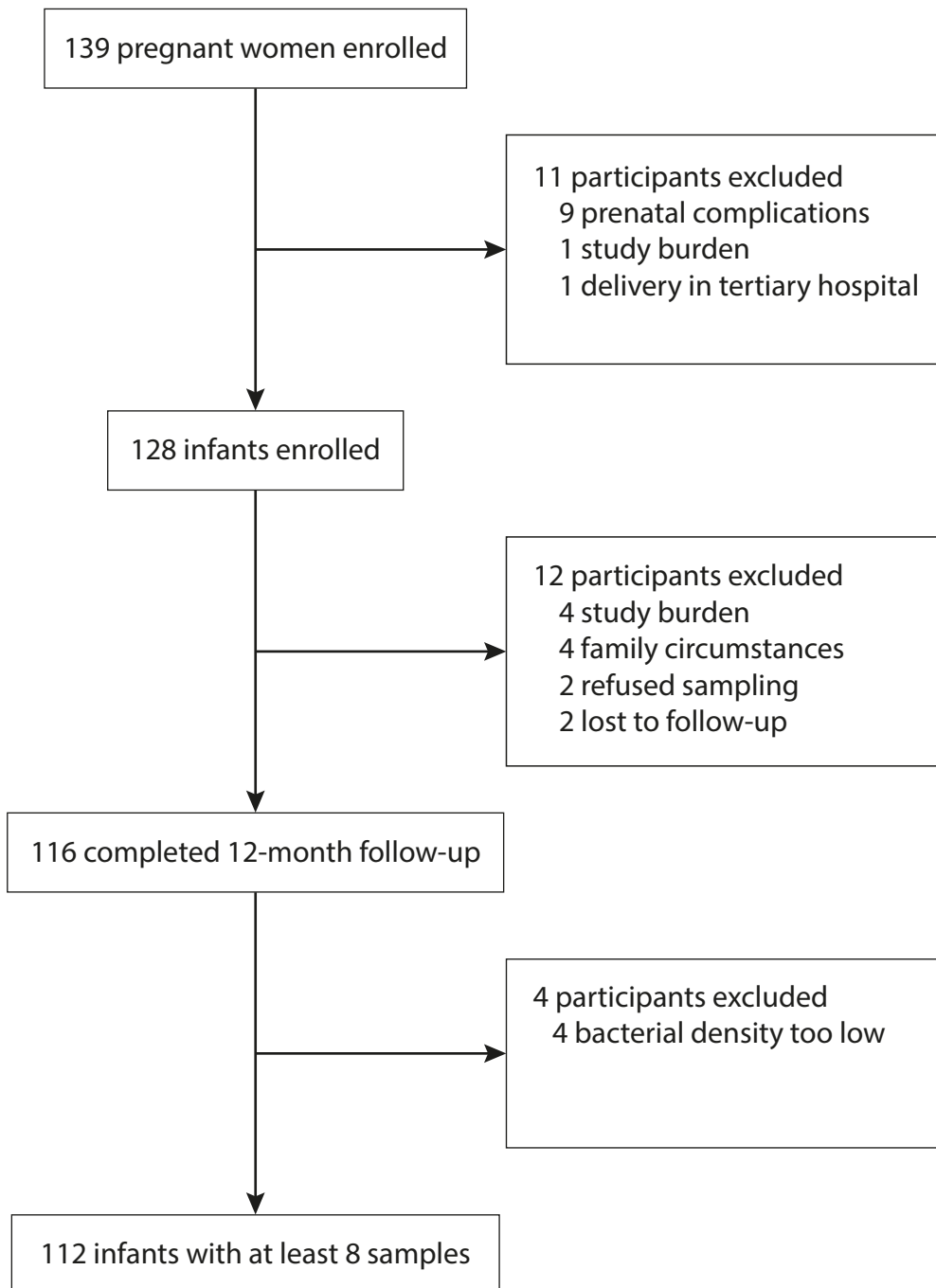


Figure E2

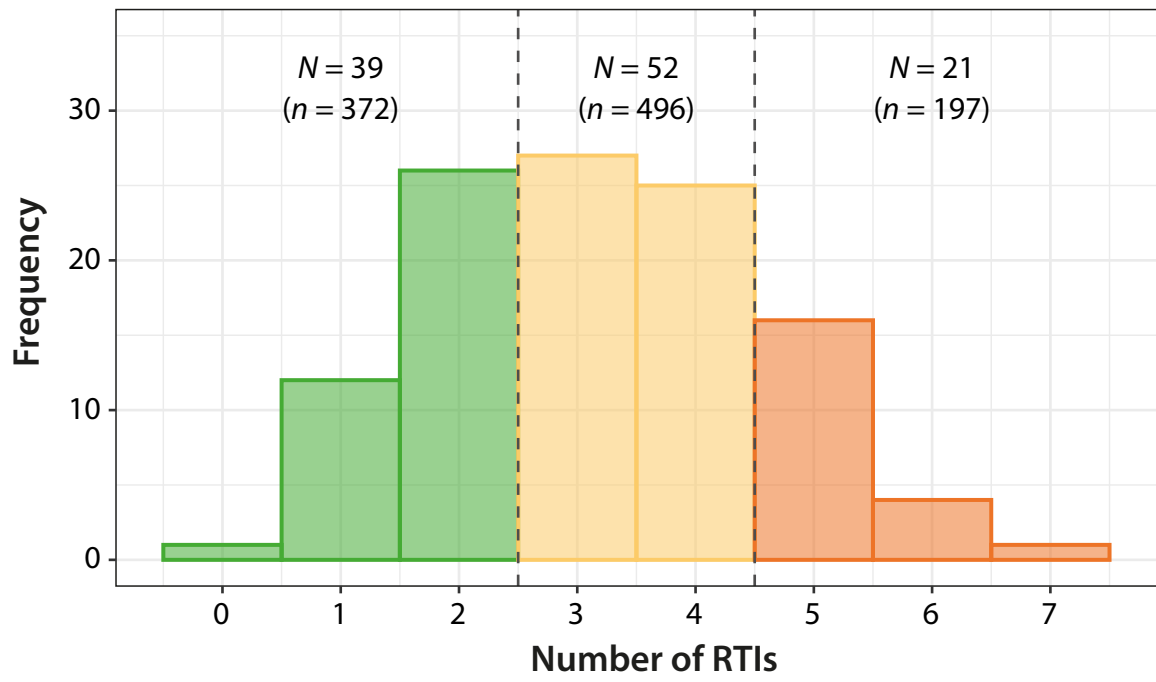
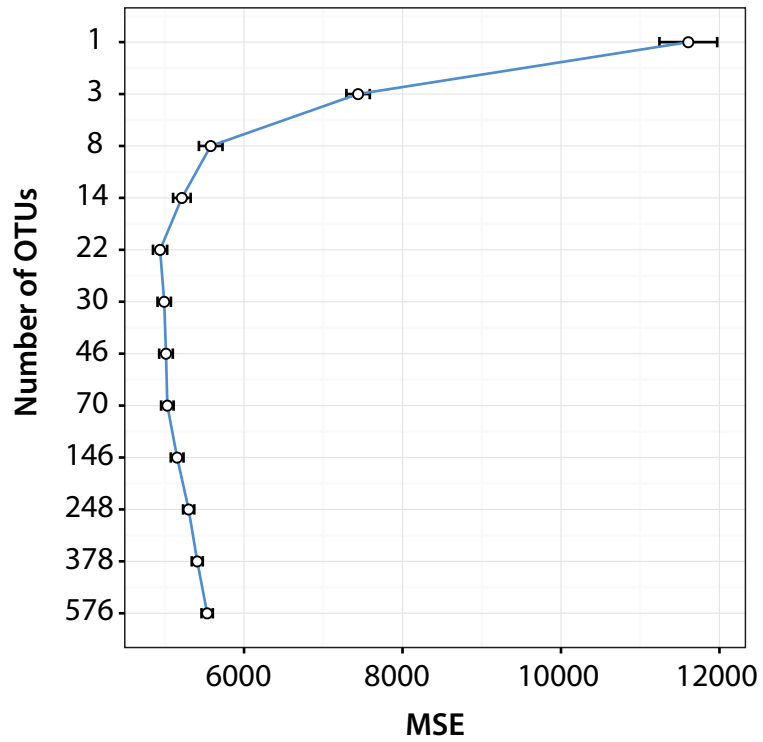


Figure E3

A



B

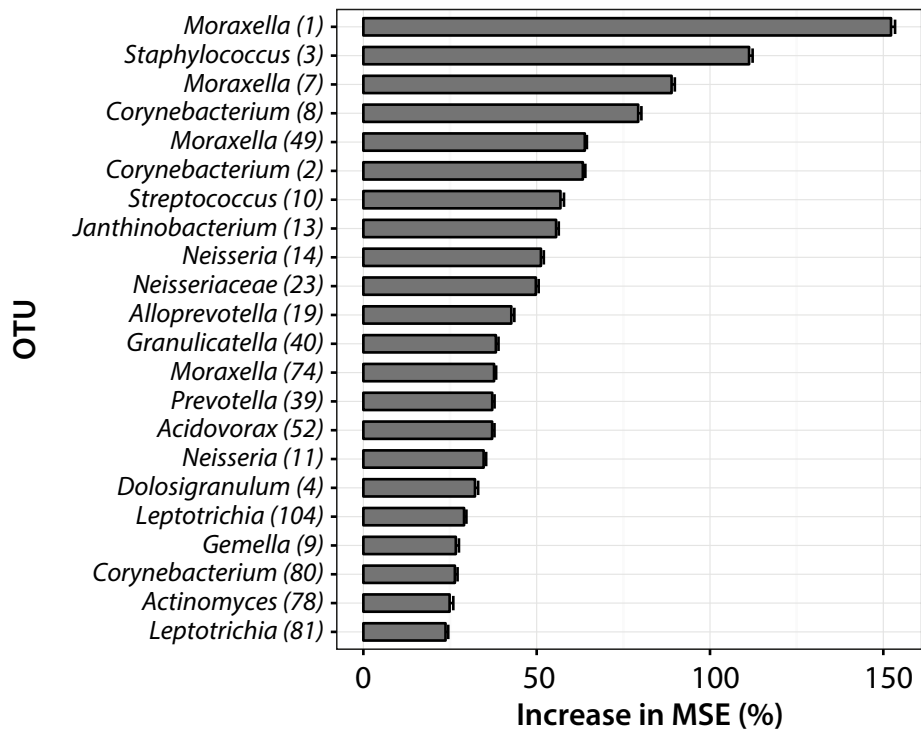
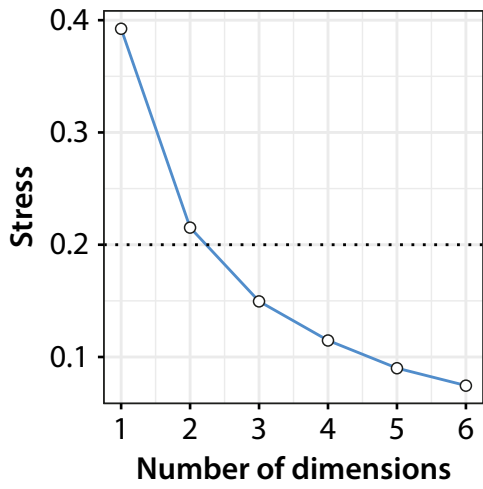


Figure E4

A



B

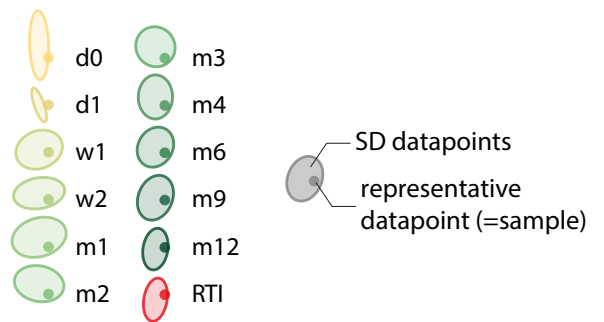
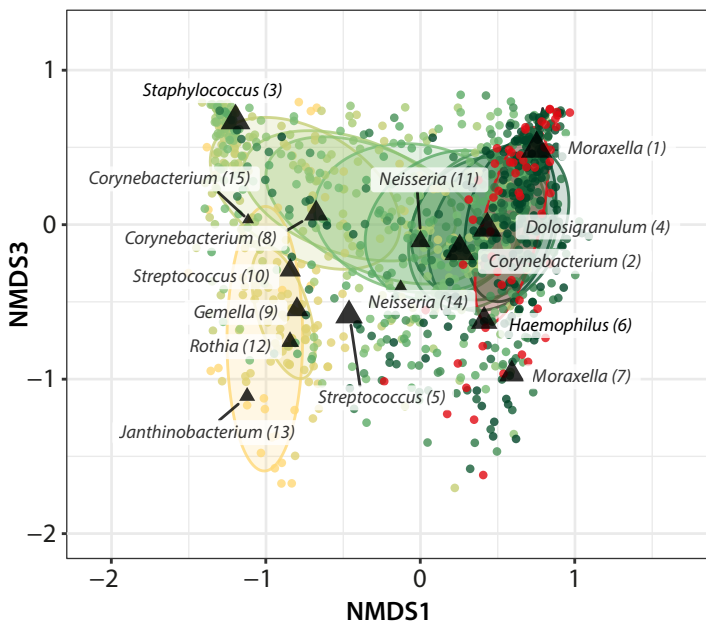
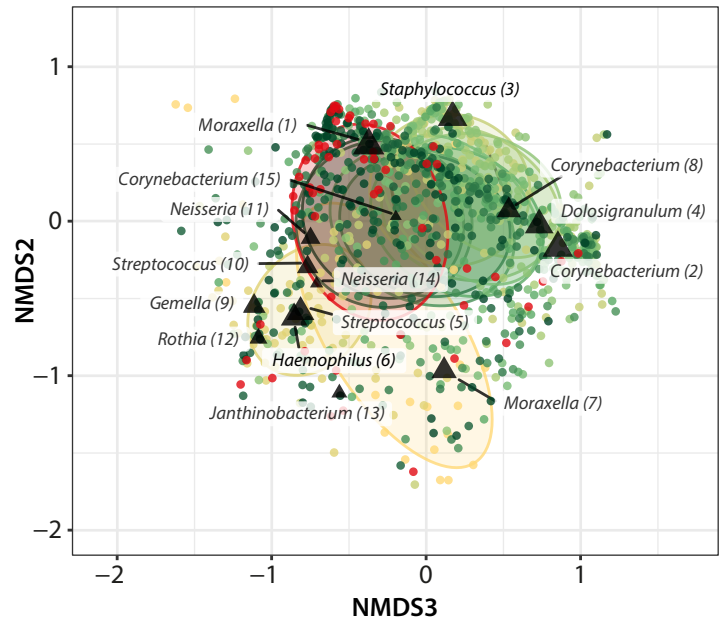
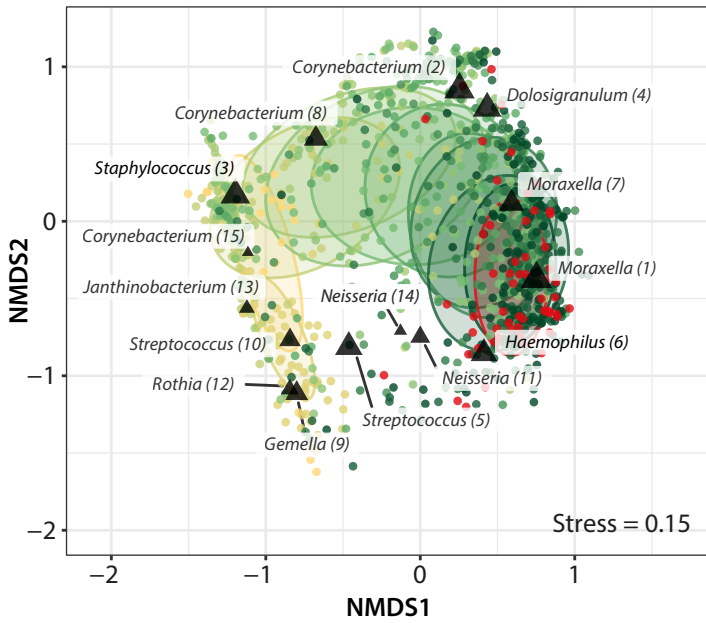


Figure E5

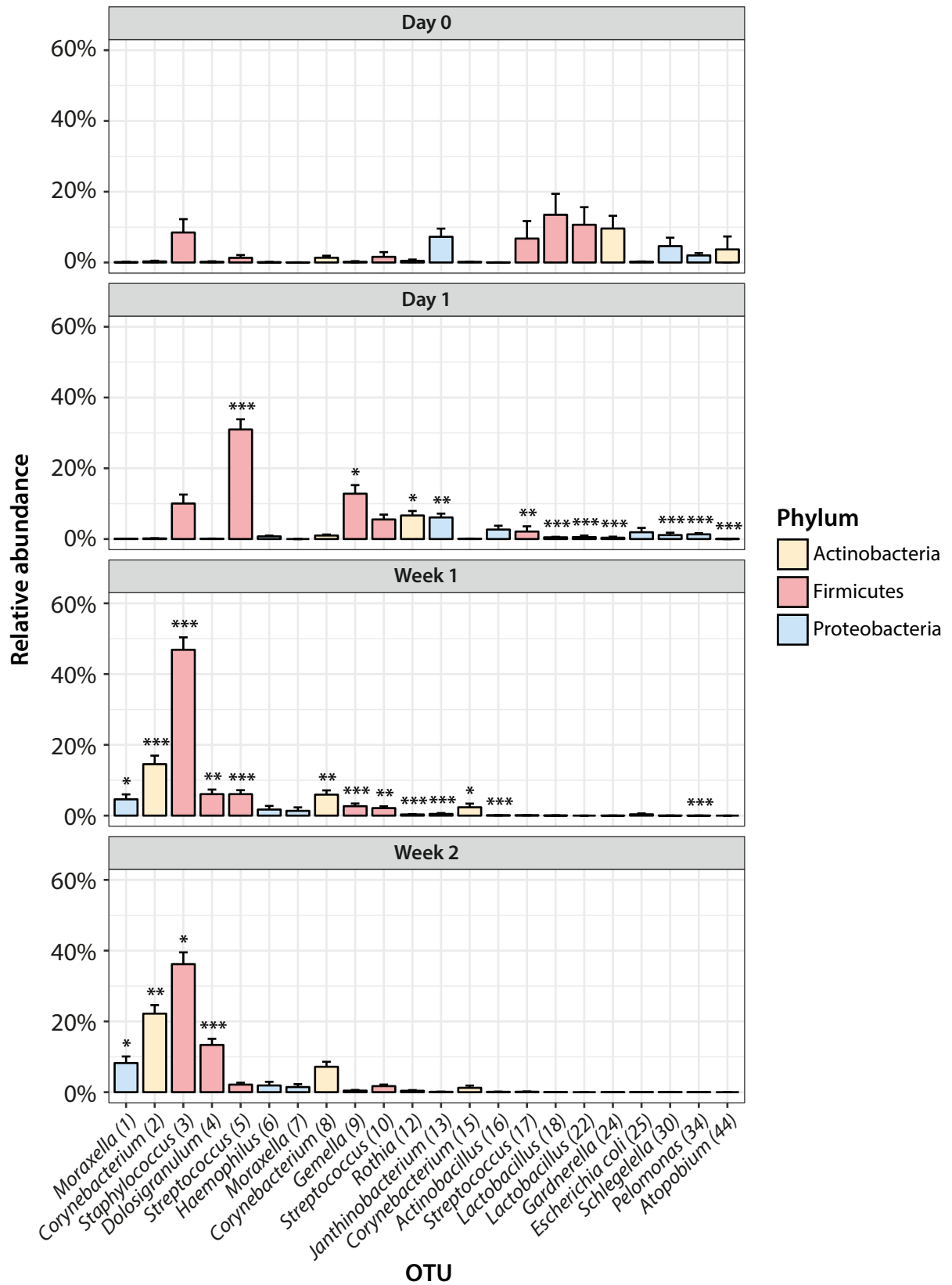


Figure E6

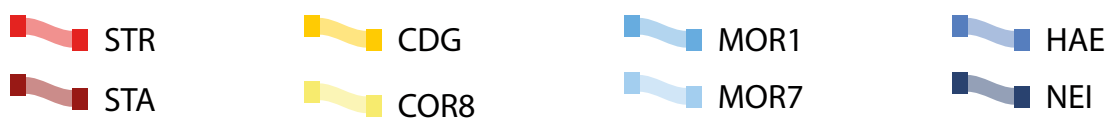
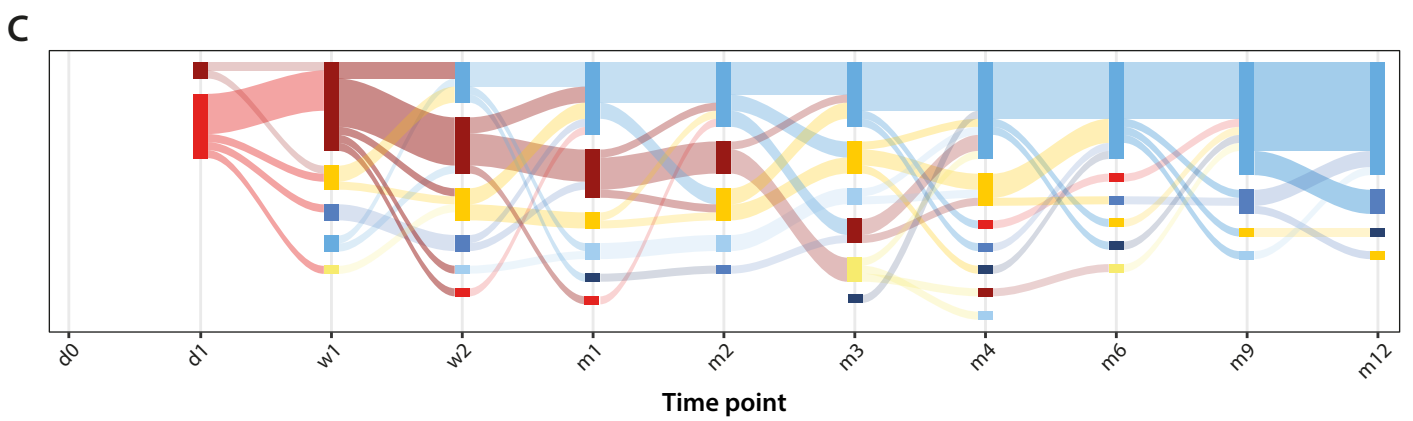
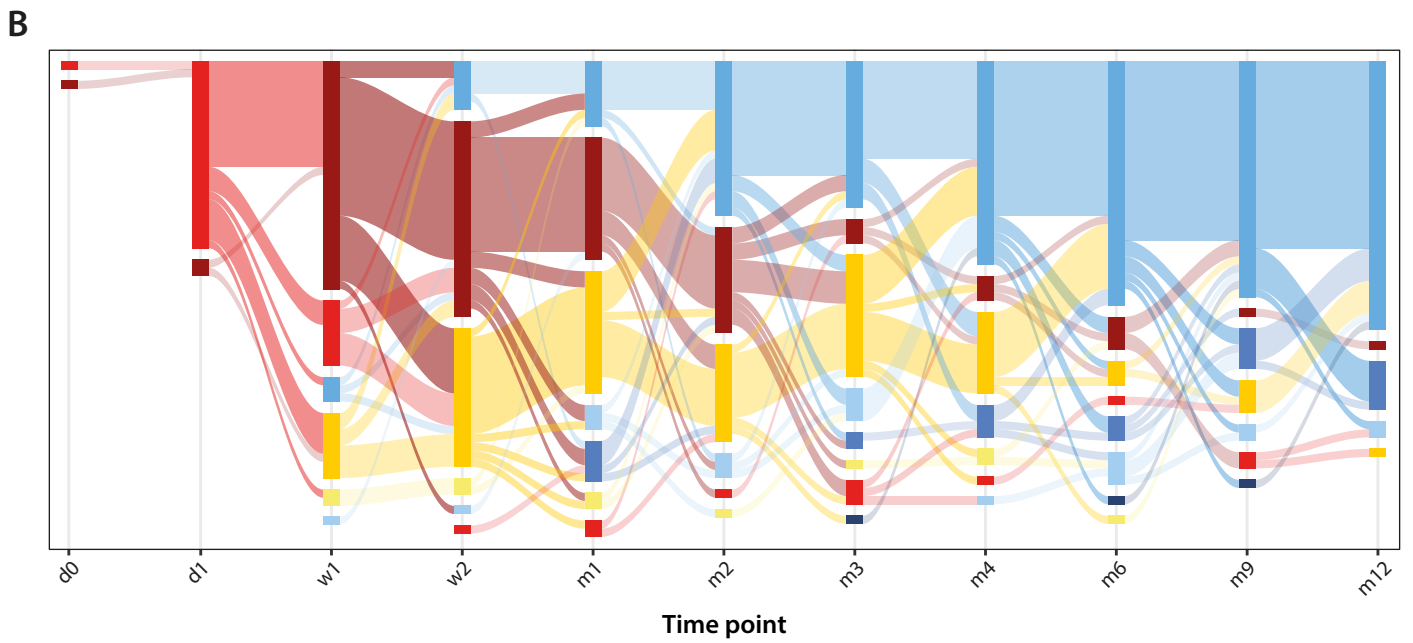
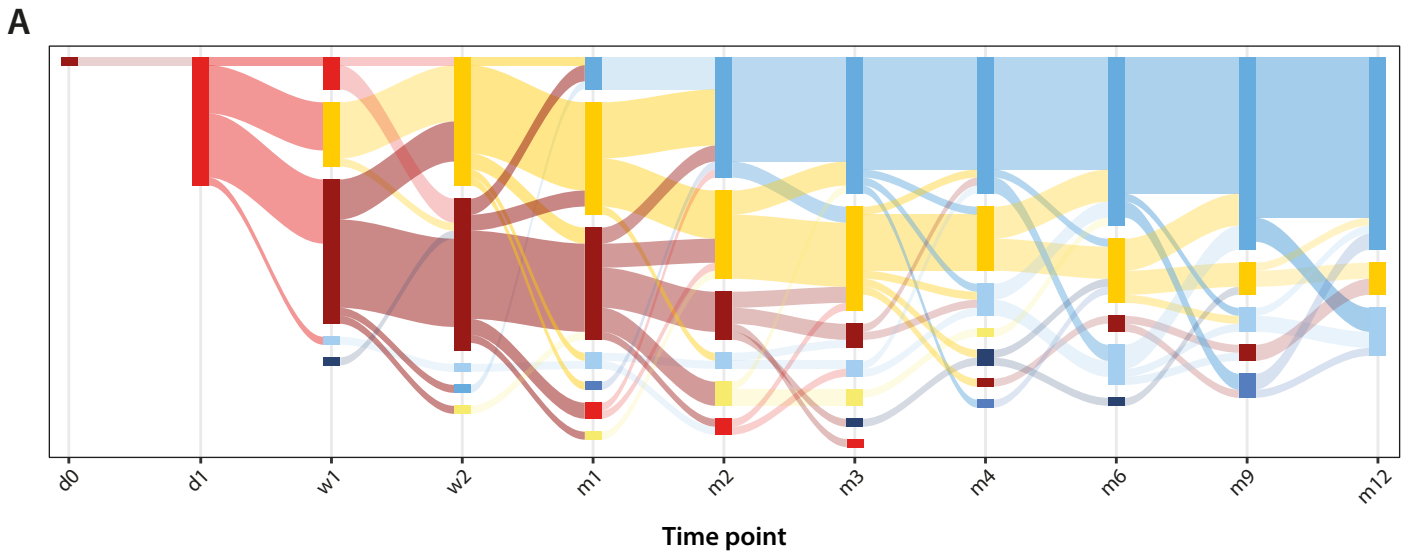


Figure E7

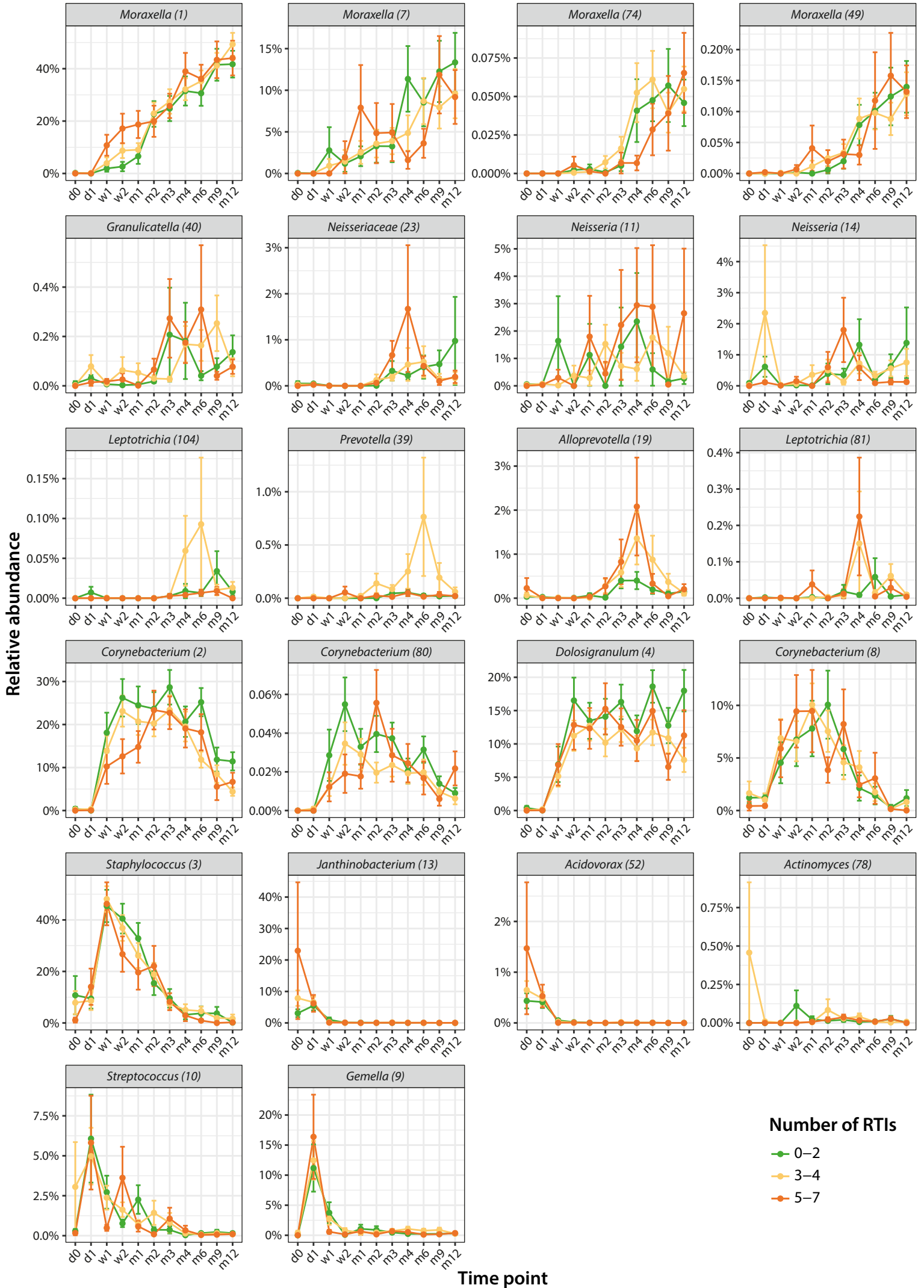


Figure E8

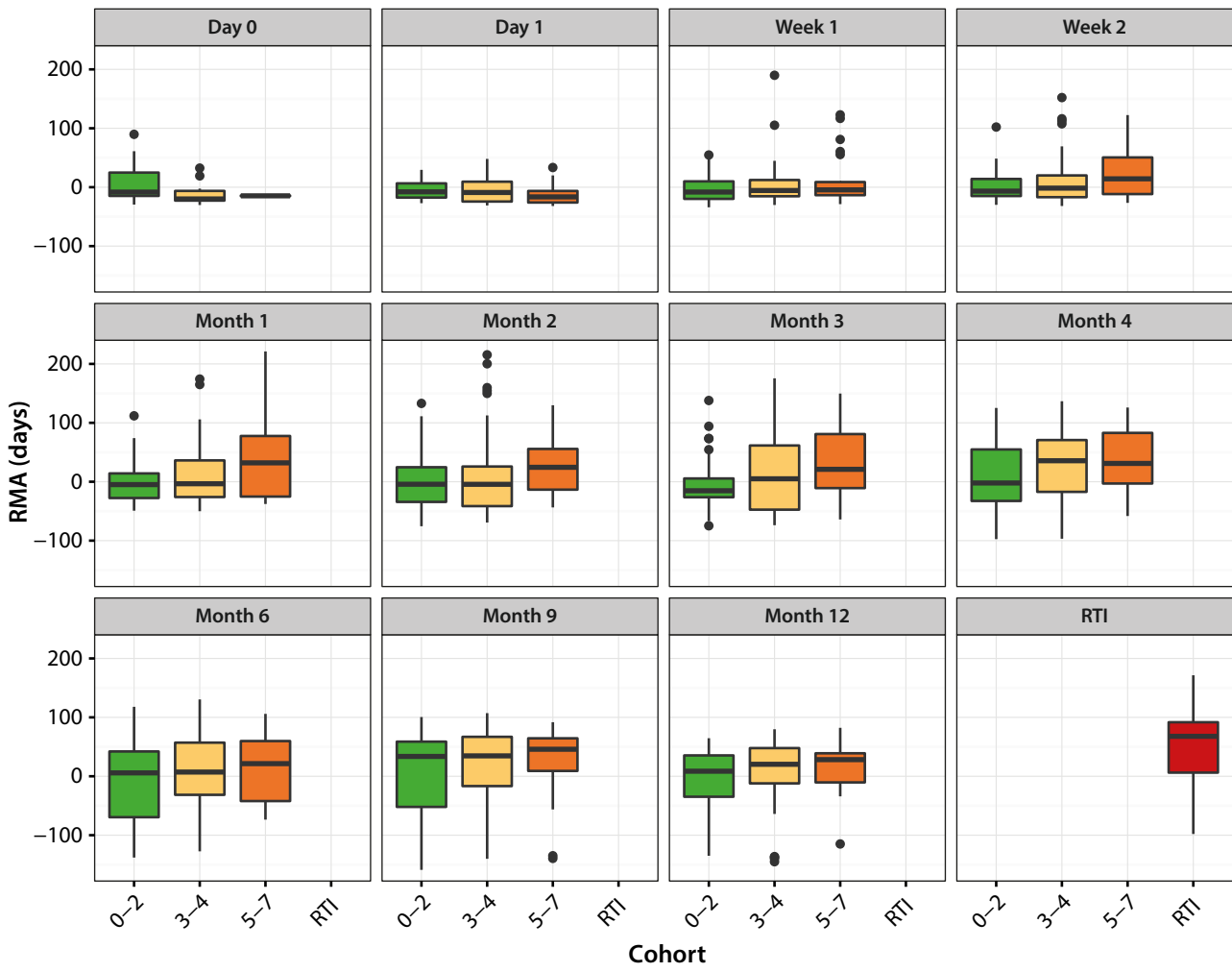




Figure E9

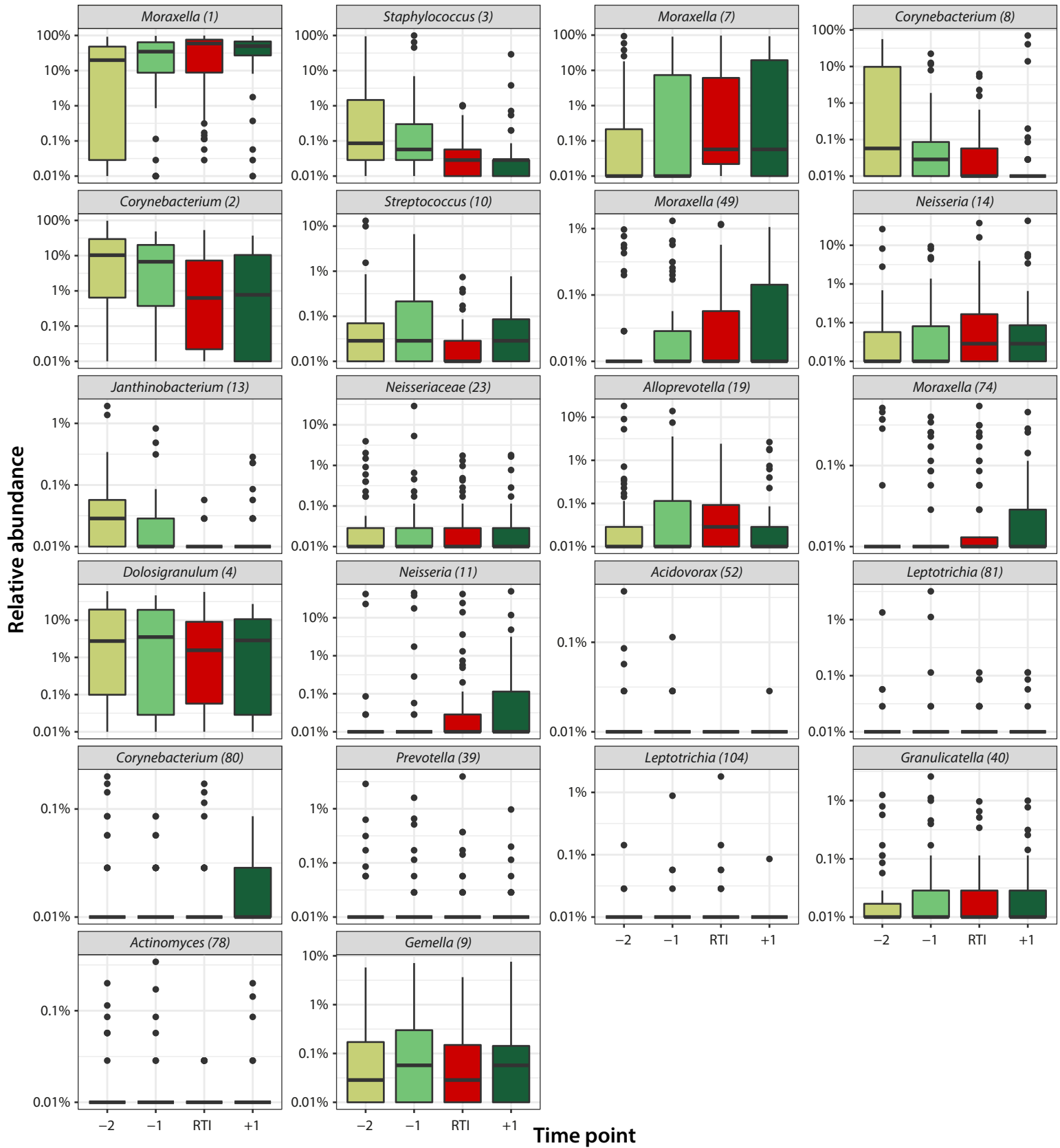


Figure E10

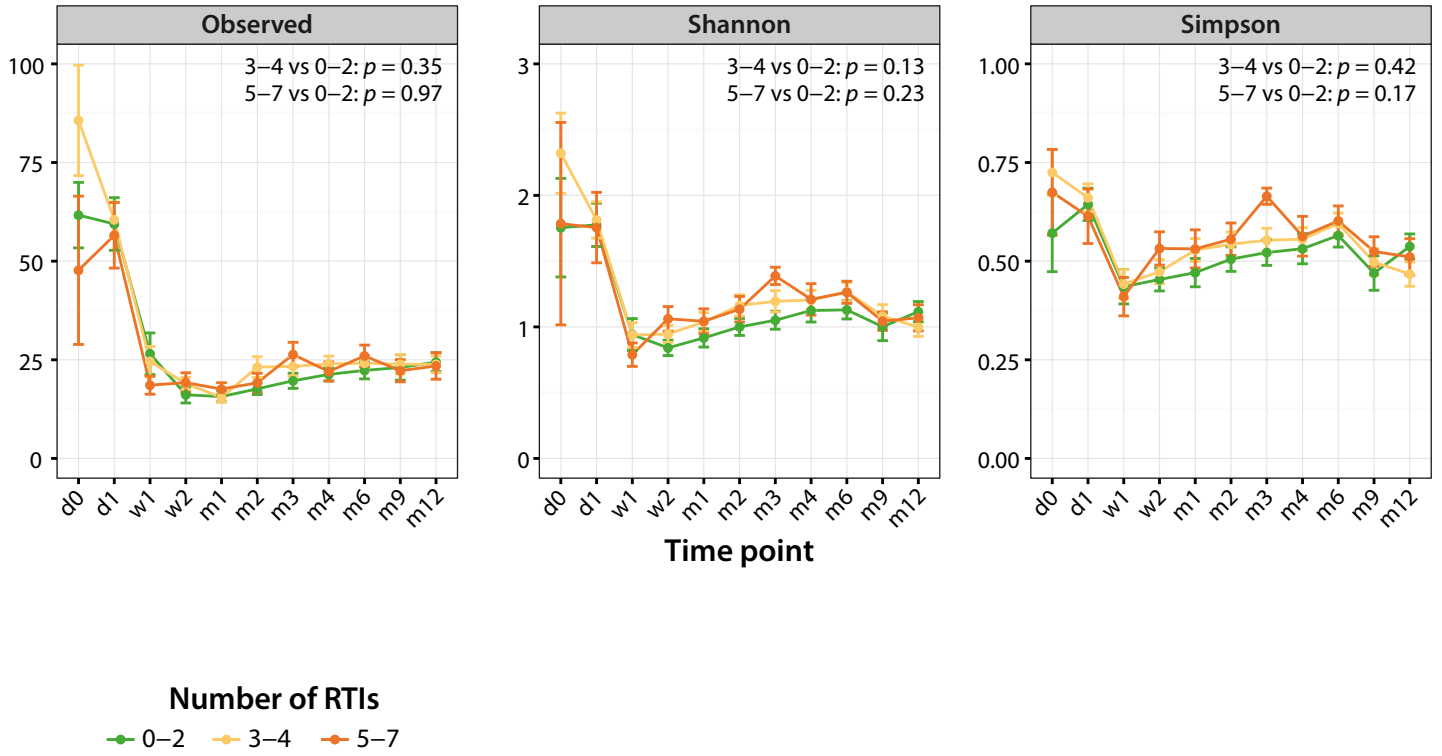


Figure E11

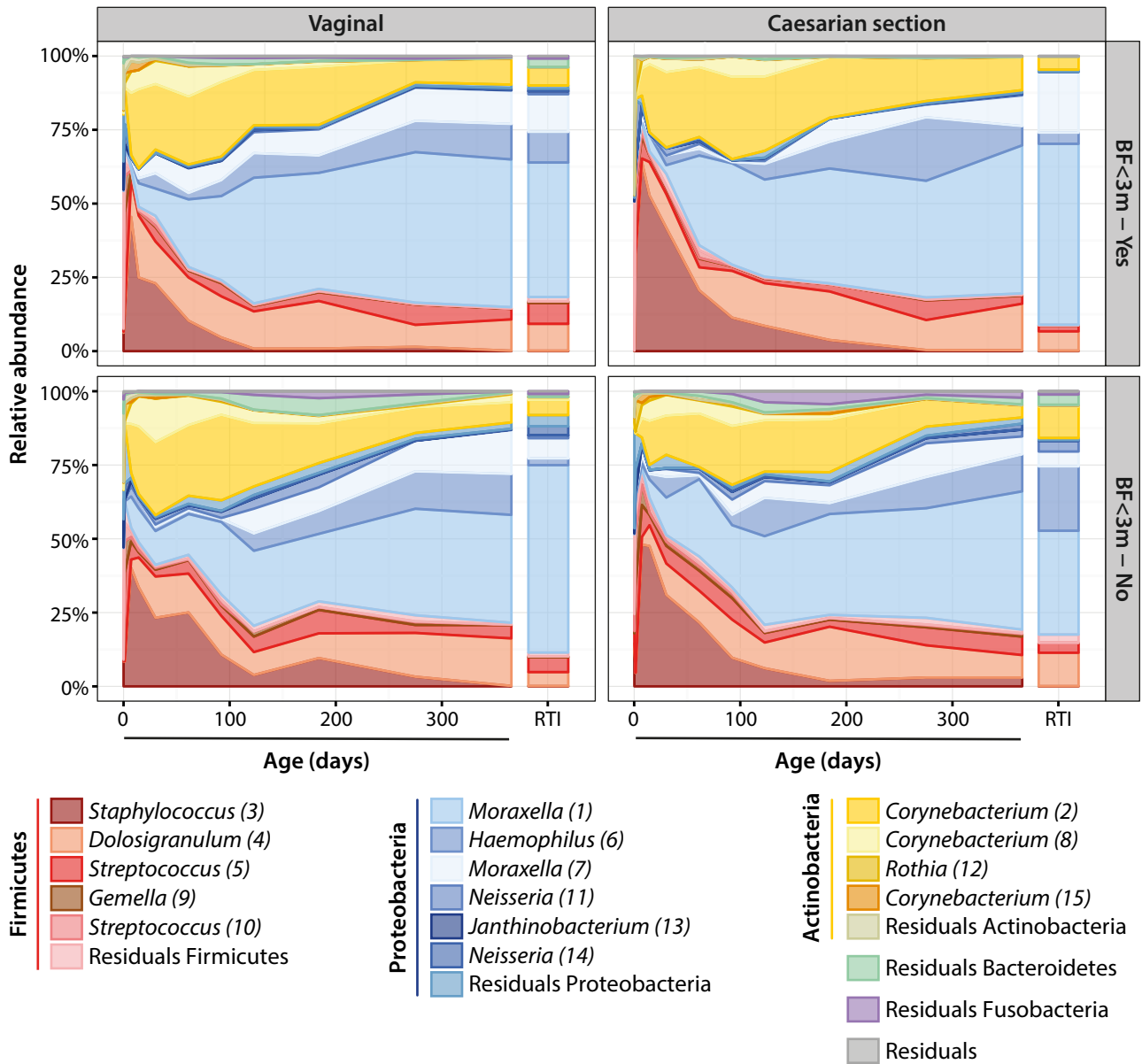
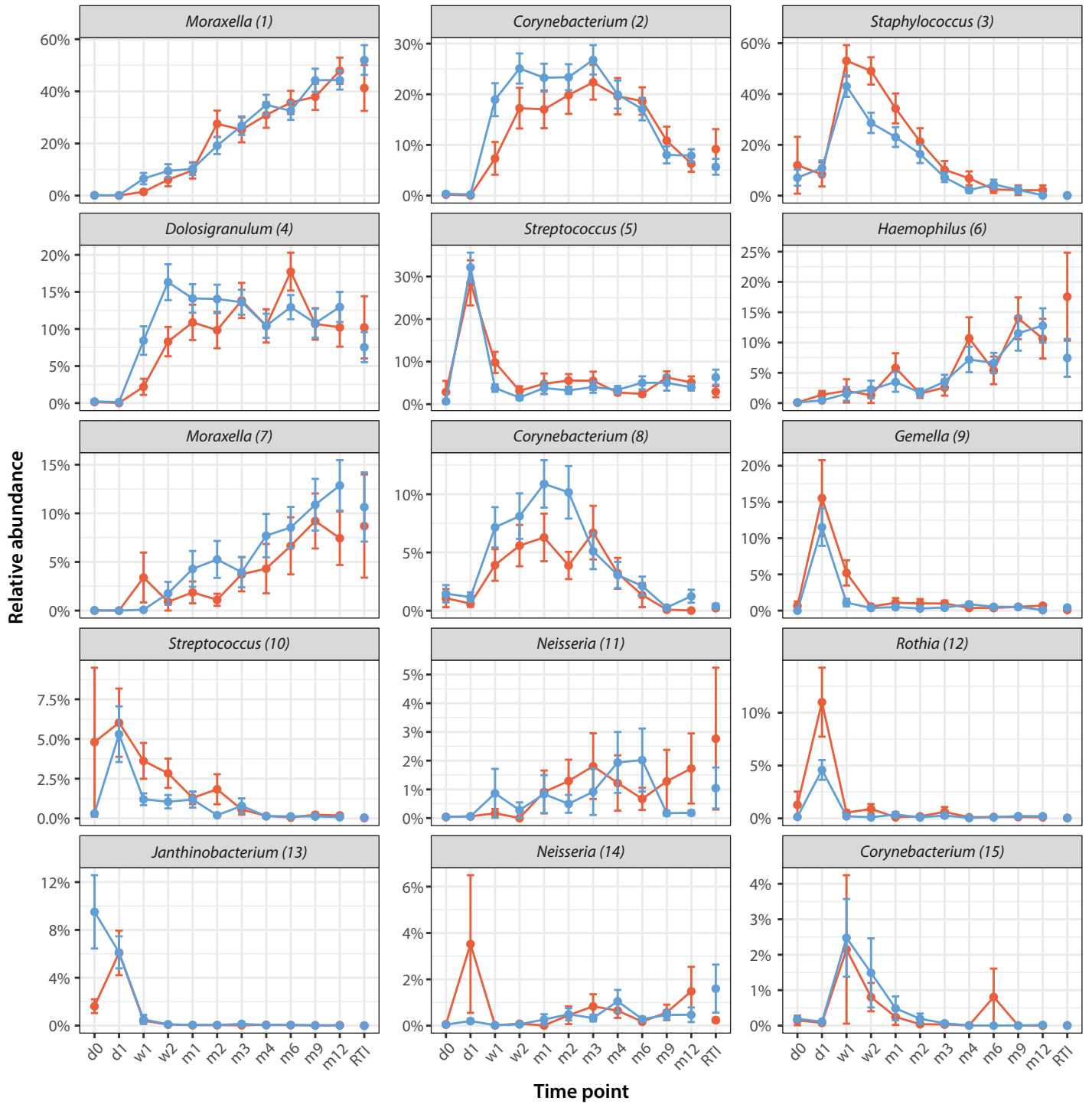


Figure E12

A



**B**

